Climate change is reducing early wet season rainfall in Puerto Rico and Jamaica

Authors

Theodore Keeping, *Centre for Environmental Policy, Imperial College, London, UK*
Mariam Zachariah, *Centre for Environmental Policy, Imperial College, London, UK*
Ben Clarke, *Centre for Environmental Policy, Imperial College, London, UK*
Claire Bergin, *ICARUS Climate Research Centre, Maynooth University, Maynooth, Ireland*
Joyce Kimutai, *Centre for Environmental Policy, Imperial College, London, UK*
Clair Barnes, *Centre for Environmental Policy, Imperial College, London, UK*
Theodore Allen, *Centre for Resource Management and Environmental Studies, University of the West Indies, Barbados*
Jayaka Campbell, *Department of Physics, University of the West Indies, Jamaica*
Zack Guido, *Arizona Institute for Resilience, University of Arizona*
Eric Harmsen, *University of Puerto Rico at Mayagüez, Mayagüez, Puerto Rico*
Dimitris A. Herrera, *Department of Geography and Sustainability, University of Tennessee–Knoxville, Knoxville, TN, USA* and *Instituto Geográfico Universitario, Universidad Autónoma de Santo Domingo, Santo Domingo, Dominican Republic.*
Héctor Jiménez-González, *University of Puerto Rico at Mayagüez, Mayagüez, Puerto Rico*
Jhordanne Jones, *Pennsylvania State University, State College, PA, USA*
William H. McDowell, *Department of Natural Resources and the Environment, University of New Hampshire, NH, USA*
Paul Miller, *University of Georgia, Athens, GA, USA*
Craig Ramseyer, *Virginia Polytechnic Institute and State University, Blacksburg, VA, USA*
Jacqueline Spence-Hemmings, *Meteorological Service, Jamaica*
Tannecia Stephenson, *Department of Physics, The University of the West Indies, Mona, Jamaica*
Michael Taylor, *Department of Physics, The University of the West Indies, Mona, Jamaica*
Julie Arrighi, *Red Cross Red Crescent Climate Centre, The Hague, The Netherlands; Global Disaster Preparedness Centre, Washington D.C., USA; Tufts University, Massachusetts, USA (based in New York, USA)*
Nick Baumgart, *Copenhagen Centre for Disaster Research; Department of Public Health, University of Copenhagen*
Karina Izquierdo Rodriguez, *Red Cross Red Crescent Climate Centre, The Hague, The Netherlands (based in Mexico City, Mexico)*
Emmanuel Raju, *Copenhagen Centre for Disaster Research; Department of Public Health, University of Copenhagen*
Mauricio Santos Vega, *Red Cross Red Crescent Climate Centre, The Hague, The Netherlands*
Adele Young, *Red Cross Red Crescent Climate Centre, The Hague, The Netherlands*
Maja Vahlberg, *Red Cross Red Crescent Climate Centre, The Hague, the Netherlands; Swedish Red Cross, Stockholm, Sweden (based in Ubmeje/Umeå, Sweden)*
Roop Singh, *Red Cross Red Crescent Climate Centre, The Hague, The Netherlands (based in New Jersey, USA)*

Friederike Otto, *Centre for Environmental Policy, Imperial College, London, UK*

Review authors

Sjoukje Philip, *Royal Netherlands Meteorological Institute (KNMI), De Bilt, The Netherlands*
Chris Boyer, *Red Cross Red Crescent Climate Centre, The Hague, The Netherlands (based in Washington, USA)*

Cite as Keeping, T. et al. (2026): Climate change is reducing early wet season rainfall in Puerto Rico and Jamaica (WWA scientific report No. 91) World Weather Attribution. DOI: 10.25560/132363

Main findings

- Caribbean vulnerability to drought results from the convergence of several compounding factors. Small island territories are naturally limited in freshwater resources and storage, increasing their vulnerability to droughts. These environmental challenges are intensified by human and tourism demands, which vary with tourism seasons, urban growth, and agricultural needs. Outdated water infrastructure, especially vulnerable drinking water systems with high leakages, worsen shortages during droughts.
- Droughts have wide-ranging impacts on agriculture including increasing crop stress, reduced yields, and reduced pasture and forage availability for livestock. Limited land on small islands means that farmers have few alternative options and often resort to expensive imported feed or selling livestock to cope. This can also contribute to food insecurity on islands that already have very high food costs.
- Before estimating any trends in the observations, we tested the influence of natural variability, comparing the performance of ENSO, NAO and AMV as covariates – all of which are known to influence Caribbean seasonal precipitation. Across regions, the December-February (DJF) NAO best improved model performance.
- Drought conditions differ across the three regions in terms of rarity, with the rarest low rainfall event of 50 years in Puerto Rico. Conditions were also rare in Jamaica with a 30 year return period.
- Warmer temperatures increase drought severity due to higher evaporation, with this year's seasonal temperatures observed to have been extremely rare before human-caused climate change. We account for this using effective precipitation, the total rainfall minus the evaporation we approximate would occur with unlimited surface water availability. May to July effective precipitation was a 15 year event in Puerto Rico, and a 30 year event in Jamaica.
- In Jamaica, observations showed a decreasing trend in both May-July actual precipitation and effective precipitation, but the strength of the decrease depends on the dataset. In Puerto Rico, a decreasing trend is observed in early wet season precipitation (pr-MJJ) and in one of the datasets for effective precipitation (eff-pr-MJJ), and is not as strong as in Jamaica. Stations from Puerto Rico show a spatially diverse trend, with strong decreases in precipitation in some regions but not in others.
- In order to assess the role of human-induced climate change in the observed drying, we combined observational data sets with climate models. In all cases, the climate models do show a small, but consistent, drying. For Jamaica, combining models and observations shows a decrease in rainfall of about 6% due to human induced climate change. An event with similar low effective precipitation as observed in 2026 is now 40% more likely compared to a 1.4°C cooler climate. For Puerto Rico the picture is very similar, with a decrease in rainfall of about 9% and an effective precipitation event that is now about 30% more likely than in a pre-industrial climate.

- We also analysed the Lesser Antilles, though sparse weather stations and the small size of the islands meant that results were highly uncertain, a minor wetting trend was seen in observations and minor drying trend in models.
- Across all regions, modelled trends were stronger with a further +1.4°C warming. Jamaica, Puerto Rico and the Lesser Antilles were all projected for an event this rare to have a further 10% lower rainfall. The effective precipitation event was projected to increase in likelihood by 3 times in Jamaica, and 2.5 times in Puerto Rico.
- Early wet season rainfall is a critical recharge period for Caribbean islands, with deficits possibly resulting in long term socioeconomic impacts on agriculture and tourism. Low early season rainfall exacerbates vulnerability, such as landslides with heavy rainfall or higher severity if drought conditions continue.
- Long-term Caribbean water sector adaptation combines modern monitoring, infrastructure and technologies such as desalination and rainwater harvesting, with long-established Indigenous and local knowledge such as seasonal water rationing, and place-based watershed stewardship. Although some components of an integrated approach to water sector management are already in use, e.g. Jamaica's expanding water monitoring system, key practices such as rainwater harvesting are underutilised relative to their potential. Water sector mitigation and adaptation may be strengthened across the region by scaling up local or decentralized water solutions and formally incorporating traditional knowledge and practices into water resource governance, planning, and resilience strategies.

1 Introduction

The year 2026 has seen widespread drying across Puerto Rico and the wider US Caribbean, following wetter than normal conditions in late winter and early-spring. Dry conditions persisted throughout May, June and July, with the region experiencing near-record high temperatures alongside low rainfall, leading to critically low streamflow in rivers, and depleting water availability due to declining water levels in reservoirs and wells.

In Puerto Rico, declining surface and groundwater have led to water-rationing for agricultural users in the south-central and southwestern regions, and for residents in parts of the San Juan metropolitan region, where 180,000 homes are currently affected (Nation of Change). There was also a surge in the number of brushfires, with more than 300 incidents recorded in July alone (Drought.gov, 23 July, 2026). Drying soils have intensified vegetation stress, particularly along the southern coast.

Similar conditions have affected the U.S. Virgin Islands, where dry soils and limited precipitation are contributing to vegetation stress and affecting specialty, row, and fruit-tree farmers. Water shortages are also preventing residents from adequately filling household cisterns (Drought.gov, 23 July, 2026).

In Jamaica, critically low rainfall and high temperatures are placing increased pressure on the island's water resources. As of August 10, major reservoirs – Hermitage Dam and Mona Reservoir – were reported to be at 40.7% and 54.5% of total capacity, respectively. Water prohibition orders have taken effect in Kingston, St. Andrew, St. Thomas, St. Mary, Portland, St. Ann, and St. Catherine, from August 17 (Radio Jamaica News Online, 17 August, 2026). This order prohibits non-essential uses of National Water Commission (NWC) water, including irrigation and watering of farms and gardens, filling ponds and swimming pools, washing vehicles with hoses, and other activities requiring excessive quantities of water. Water use is restricted primarily to essential domestic needs such as drinking, cooking, washing, bathing, and sanitation.

The drought onset against the backdrop of Saharan dust outbreaks and a developing El Niño, with the latter expected to intensify and persist for the rest of 2026. Frequent Saharan dust intrusions can suppress rainfall, increase dryness and contribute to higher temperatures, while El Niño may further disrupt normal rainfall patterns and intensify heat. Together, these conditions may lead to prolonged dry spells, reduced water availability, agricultural losses and an increased risk of wildfires. As the 2026 mid-summer dry season progresses, communities already experiencing drought could face growing pressure on water supplies, food security and livelihoods.

1.1 Impacts

Across the insular Caribbean, prolonged rainfall deficits, above average temperatures, and declining soil and water availability have generated widespread impacts across agriculture, water resources, ecosystems, and livelihoods (NIDIS, 2026).

In Puerto Rico, reservoirs, streams, and groundwater levels have declined substantially, prompting agricultural water rationing, including restrictions to three days per week in parts of the southwest. Some wells have reached critical levels, while reduced streamflow has affected irrigation and local water availability (NIDIS, 2026). Farmers report cracked and moisture deficient soils (see Figure 1.1.1), crop stress and delayed growth, premature fruit ripening, and losses among coffee, citrus, plantains, bananas, breadfruit, and other fruit trees. Pasture deterioration has reduced forage availability, increasing reliance on purchased fodder and depleting hay reserves.

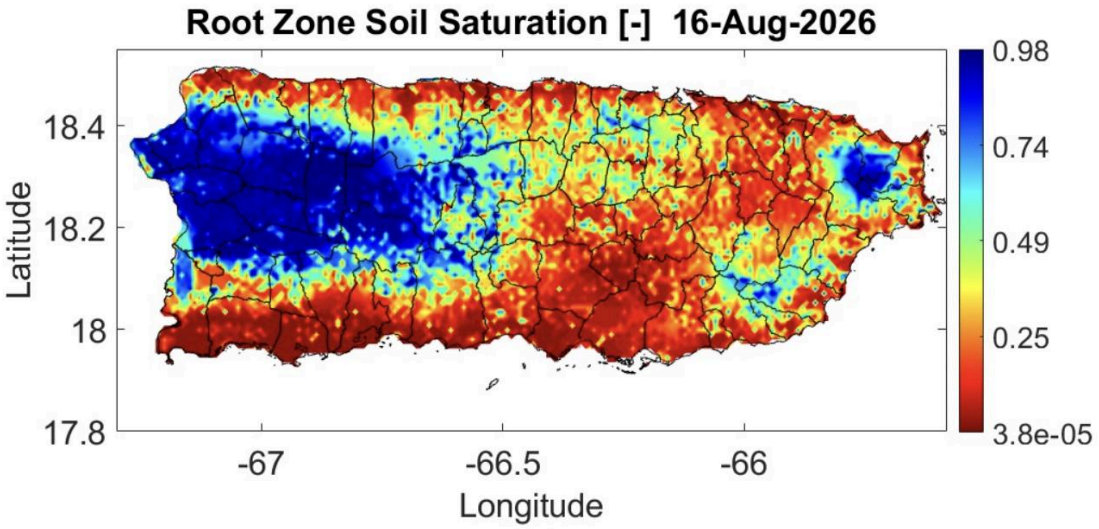


***Figure 1.1.1**: Root zone soil saturation over Puerto Rico (Harmsen et al., 2021).*

Livestock and poultry producers in the U.S Virgin Islands similarly face declining pasture and water availability, alongside rising production costs (NIDIS, 2026). Vegetation stress and forest defoliation are widespread, while some young trees and crops have died. Depleted ponds, groundwater constraints and insufficient precipitation have limited both agricultural and household water supplies.

In Jamaica at the end of July there were seven parishes reporting agricultural drought including the bread-basket parish of St. Elizabeth, and severely reduced available water supplies have led to scheduled restrictions in parts of Kingston and St Andrews. From 17 August, non-essential use of National Water Commission supplies was prohibited across seven parishes, including restrictions on agricultural irrigation (JIS, 2026). Farmers also require emergency water deliveries and report crop damage across cabbage, yam, lettuce, and potentially plantain and banana.

Dry conditions have also increased wildfire risk, with nearly 300 reports in Puerto Rico during the period, including fires affecting agricultural areas and infrastructure. Persistent drought is expected to compound these impacts through autumn, with below-normal precipitation and above-normal temperatures are forecast (NIDIS, 2026).

1.2 Drought Events in the Caribbean

Climate warming and climate variability are increasingly intensifying water stress and drought risks across the Caribbean, with significant implications for water resources and agriculture. Human-induced warming has contributed approximately 15–17% to the 2013-16

pan-Caribbean drought severity through increased evapotranspiration and has influenced the extent of drought-affected land (Herrera et al., 2018).

El Niño Southern Oscillation (ENSO) variability further influences rainfall patterns in the Caribbean region, but the strength and direction of the rainfall signal vary by island, season, and subregion. In Jamaica, El Niño is associated with lower totals of wet season heavy rainfall (Avalon-Cullen et al., 2024). Puerto Rico's rainfall and drought records show only a weak ENSO signal and no major ENSO control on monthly, seasonal, or annual rainfall (Torres-Valcárcel 2018). Future climate projections indicate increasing crop water stress in Puerto Rico and St. Croix, particularly from the mid-century onward, with temperature changes potentially exerting a greater influence than reduction in precipitation on crop water requirements (Morares et al., 2023). These findings highlight the vulnerability of Caribbean islands to precipitation deficits and water stress and emphasize the need for water management, agricultural adaptation, and climate-resilience strategies.

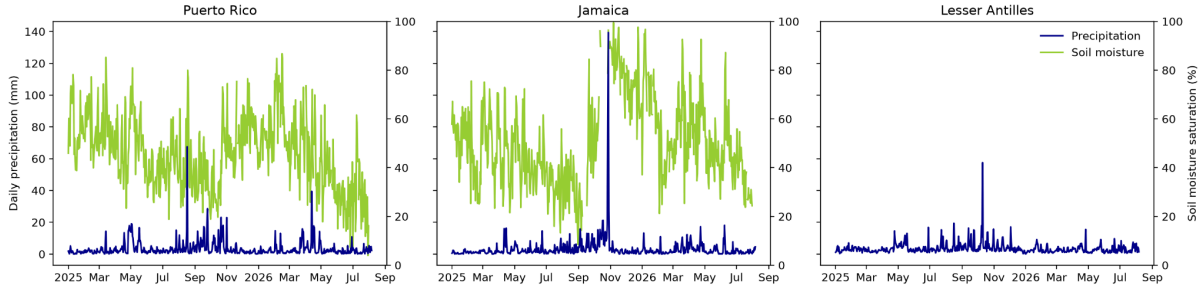


Figure 1.2.1: *Daily precipitation (blue lines) and soil moisture saturation (green lines) from January 2025 to August 2026, averaged over small islands in the Caribbean: Puerto Rico, Jamaica and the Lesser Antilles. Precipitation data from MSWEP, satellite-derived soil moisture data from SM v202312 global soil moisture dataset.*

Figure 1.2.1 shows daily precipitation (in blue) and soil moisture saturation (in green) over the islands of Puerto Rico, Jamaica and the Lesser Antilles. Soil saturation data are not available over the Lesser Antilles due to their size and the resolution of the *SM v202312* dataset, which is unable to represent these small islands. In Jamaica and Puerto Rico, soil saturation increases in the short term following rainfall - particularly following extreme rainfall events like passing or landfalling hurricanes - and declines over time as the soil drains and moisture is lost to evapotranspiration. During the first ten days of August (the period for which satellite soil moisture data were available at the time of writing) the average daily soil saturation was below 20% in Puerto Rico and around 25% in Jamaica.

1.2.1 Jamaica

Jamaica experienced a marked deterioration in rainfall during the early rainfall season of 2026, resulting in meteorological drought across several parts of the island. In June, 10 of 13 parishes recorded rainfall below their 1991–2020 climatological means, with deficits of 16–45%. Islandwide, rainfall averaged 114 mm, approximately 94% of the June

climatological mean. More significant than this islandwide total was the widespread and rapid drying evident in the May–June Standardized Precipitation Index (SPI): all 13 parishes recorded negative SPI values and 12 deteriorated relative to the preceding period, with conditions ranging from near-normal dry to extremely dry. By May–July, the three-month SPI (SPI-3), indicative of agricultural drought, showed drought conditions in seven parishes, including the important "breadbasket" parish of St. Elizabeth. This deterioration occurred during the climatologically important early rainfall season, reducing opportunities to replenish soil moisture, surface-water storage and groundwater ahead of the normally drier mid-summer period. The August–October outlook indicates that recovery may be constrained, with below-normal rainfall favoured across much of Jamaica.

The drought is occurring against a backdrop of substantial hydroclimatic variability in Jamaica. The island has a strongly bimodal rainfall cycle, with an early rainfall season, a mid-summer minimum, and a later rainfall season from September to November. Interannual and decadal variability, including ENSO, can strongly influence rainfall. Jamaica has experienced several significant droughts in recent decades, including 2004/05, 2009/10 and 2014/15, while long-term observations show warming and changes in rainfall variability. Failure of the early rainfall season is particularly consequential because it can leave water resources and agriculture more exposed to rainfall deficits during the subsequent mid-summer dry period.

1.2.2 Puerto Rico

In Puerto Rico, water stress varies spatially, with southern regions experiencing greater baseline stress because of reduced net infiltration within the rain shadow of the Cordillera Central, while drought conditions increasingly affect central and eastern areas through reduced precipitation and infiltration, higher evapotranspiration, and limited groundwater availability (Morares et al., 2023).

Previous significant droughts in Puerto Rico include 1994 and 2015, with the latter marking the first instance of "extreme drought" over the island according to the U.S. Drought Monitor (Mote et al. 2017). Similar to the current water crisis, the 2015 drought began its rapid onset in May and was concentrated over the eastern portion of the island. Later analyses tied the development of the drought to an active Saharan air layer (SAL) (Dolce et al. 2025), which produced persistently stable conditions (Mote et al. 2017) and has been shown to suppress precipitation over the island (Miller and Ramseyer 2024).

1.3 Event Definition

In this report, we study the influence of anthropogenic climate change by comparing the likelihood and intensity of similar early wet season precipitation (May-July precipitation, pr-MJJ) and early wet season effective precipitation (May-July precipitation minus potential evapotranspiration, eff-pr-MJJ) at present with those in a 1.4°C cooler climate without

human-caused warming (based on Forster et al., 2026). Precipitation and effective precipitation are referred to as meteorological and ecological drought through this report. We also extend this analysis into the future by assessing the influence of a further 1.4°C of global warming from present. This is in line with the latest Emissions Gap Report from the United Nations Environment Programme, which shows that the world is on track for at least 2.8°C temperature rise given currently implemented policies (UNEP, 2025).

We focus on three study regions (see Figure 1.3.1) the larger islands of Jamaica and Puerto Rico which are both in severe drought, as well as the Lesser Antilles island chain where the US Virgin Islands, St Kitts, St Lucia, St Vincent, and Grenada are all undergoing droughts (CariCOF, 2026).

Note that the effective precipitation measure does not directly reflect the moisture flux from precipitation and evapotranspiration, but rather uses the potential evapotranspiration (PET). PET assumes unlimited moisture availability at the ground surface, whereas in reality evaporation decreases as moisture is depleted and plants stop transpiring in dryer and hotter conditions. PET was calculated according to Hargreaves and Samani (1985) – which assumes a simple relationship with daily maximum and minimum temperatures, and was developed using closely cropped vegetation. As covered in Kimutai et al. (2025), whilst temperature-only derivations of PET are subjective and often less accurate than schemes accounting for radiation, wind and humidity – they are often superior in regions where these ancillary variables are either unreliable or not available.

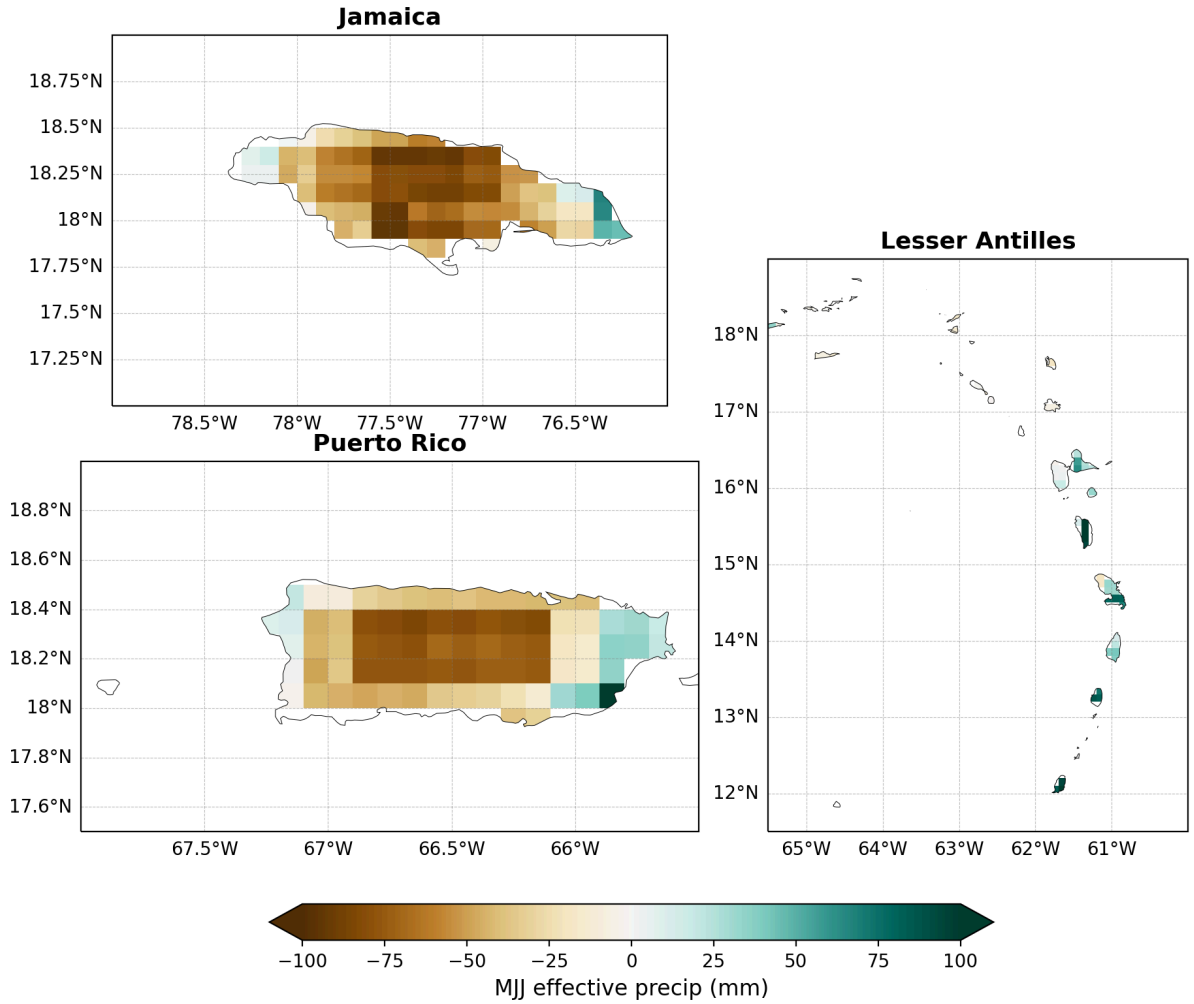


Figure 1.3.1*: overview of the three study regions considered in this analysis, with the MJJ precipitation minus potential evapotranspiration (calculated according to* Hargreaves and Samani, 1985*) shown according to MSWEP to illustrate observed drought drivers. See Appendix A0 for a more detailed overview of Puerto Rico's precipitation derived from station data.*

2 Observed trends

2.1 Trends in gridded and station data

The return period estimates in observation-based datasets with the event included are 30 years for Jamaica – for both meteorological and ecological drought; 50 years for meteorological drought in Puerto Rico and 15 years for ecological drought; and 5 years for both types of drought in the Lesser Antilles (Table 2.1.1). Only MSWEP/MSWX was used to estimate return periods, as CHIRPS/CHIRTS was not updated to include the full period of the 2026 event. We note that the choice of return period affects the estimated probability ratios but that the estimated changes in intensity are independent of this. The results for the

observational datasets evaluated at these return periods are shown in Tables 2.1.2.1, 2.1.3.1, and 2.1.4.1.

Table 2.1.1: Magnitudes and estimated return period of May-July meteorological (pr-MJJ) and ecological (eff-pr-MJJ) drought for 2026 in Jamaica, Puerto Rico and the Lesser Antilles according to MSWEP/MSWX, with the take return period used in the analysis included below.

		Jamaica	***Puerto Rico***	***Lesser Antilles***
pr-MJJ	MSWEP	28.5 (6.87, Inf)	50.7 (14.5, Inf)	5.57 (2.93, 127)
	Chosen	***30***	***50***	***5***
eff-pr-MJJ	MSWEP/MSWX	27.2 (2.70, Inf)	14.1 (4.89, Inf)	4.03 (2.06, Inf)
	Chosen	***30***	***15***	***5***

2.1.1 Influence of modes of natural variability

ENSO, the NAO (North Atlantic Oscillation), and AMV (Atlantic Multidecadal Variability) have all been linked to seasonal precipitation patterns in the Caribbean (Clarke et al., 2026, Stephenson et al., 2014, Taylor et al., 2002, Giannini et al., 2001, Herrera and Ault, 2017). We therefore tested the performance of models where these were included as covariates, using one index for the decadally smoothed AMV, and the concurrent 3-month index of the NAO and Niño3.4 in addition to the two prior seasonal aggregations (DJF and MAM). Tables 2.1.1.1 and 2.1.1.2 list Akaike Information Criterion (AIC) values for model fits – showing that the DJF NAO index offers the most substantial improvement in fit across regions and for both precipitation and effective precipitation. We therefore used an NAO DJF covariate in all observation and model fits, the value this year was weak (-0.11), so we do not emphasise its effects in the results.

Whilst the DJF and MAM averages of the NAO were assessed, the strength (2.69) of this year's March value was noteworthy, with the influence of that individual month's configuration on this year's drought not assessed in this report.

The NAO can influence seasonal precipitation over the Caribbean, through its influence on tropical North Atlantic SSTs and trade winds (Enfield and Mayer, 1997; Taylor et al., 2002).

Here, the index was calculated according to the standardised seasonal pressure difference between the Azores and Reykjavik.

Table 2.1.1.1: AIC values for MSWEP pr-MJJ fits for each additional covariate. The lowest AIC value is highlighted in green.

Covariates	Puerto Rico		Lesser Antilles		Jamaica	
	MSWEP	CHIRPS	MSWEP	CHIRPS	MSWEP	CHIRPS
GMST only	597.1	568.1	586.0	562.9	624.9	557.6
Nino DJF	599.8	570.3	586.4	563.2	627.1	560.8
Nino MAM	601.0	569.8	587.6	564.5	627.2	560.5
Nino MJJ	601.3	567.7	585.2	563.7	627.3	560.4
AMV	601.0	570.5	587.2	564.7	626.5	560.7
NAO DJF	590.8	560.0	575.6	555.8	626.5	560.9
NAO MAM	601.5	567.9	583.7	563.3	626.7	563.9
NAO MJJ	601.4	569.8	587.7	563.9	627.1	560.7

Table 2.1.1.2: AIC values for MSWEP eff-pr-MJJ fits for each additional covariate. The lowest AIC value is highlighted in green.

Covariates	Puerto Rico		Lesser Antilles		Jamaica	
	MSWEP	CHIRPS	MSWEP	CHIRPS	MSWEP	CHIRPS
GMST only	604.1	570.9	581.7	344.1	631.0	564.3
Nino DJF	606.9	572.4	585.3	346.4	633.7	566.7
Nino MAM	607.6	571.2	581.4	344.4	626.7	566.8
Nino MJJ	597.5	567.3	579.4	341.7	629.3	567.1
AMV	606.8	572.0	585.7	346.3	632.5	567.9
NAO DJF	606.9	566.4	580.4	335.9	624.9	567.3
NAO MAM	600.3	566.8	576.9	340.5	631.1	566.2

NAO MJJ	607.9	571.0	583.8	344.9	626.0	567.7

2.1.2 Jamaica observed trends

In Jamaica, a strong decreasing effect is seen in early wet season precipitation (pr-MJJ) and effective precipitation (eff-pr-MJJ) in MSWEP, with an uncertain effect seen in CHIRPS. A study by Clarke et al 2026 found that the rainfall reductions in early wet season are associated with the intensification and westward extension of the North Atlantic Subtropical High which acts as a rainfall suppressor over the eastern Caribbean.

The emergent drying trend in MSWEP precipitation was found to have changed in intensity by -10.2% (95% CI: −60.6% to −5.97%) with 1.4°C of climate change, with an increase in probability of the 30-year event of at least 1.4 times according to the 95% confidence interval. For effective precipitation (accounting for drying using potential evapotranspiration) the increase in probability of a 30-year event of at least 5.2 times, and a decrease in eff-pr-MJJ of -96.3mm (95% CI: −283mm to −33.2mm). In CHIRPS, the trends are not emergent, and are close to no change, with a decrease in pr-MJJ of -0.16% (95% CI: −20.4% to +33.3%) and eff-pr-MJJ of -0.4mm (95% CI: −65.9mm to −121mm).

Table 2.1.2.1: Probability ratio and change in magnitude for May-July precipitation and effective precipitation in the Jamaica study region.

	Jamaica			
	pr-MJJ		eff-pr-MJJ	
	Probability Ratio	Relative Intensity Delta (%)	Probability Ratio	Absolute Intensity Delta (mm)
CHIRPS	1.08 (0.100, Inf)	-0.158 (-20.4, 33.3)	1.07 (0.0736, Inf)	-0.437 (-65.9, 121)
MSWEP	1.63 (1.40, Inf)	-10.2 (-60.6, -5.97)	Inf (5.21, Inf)	-96.3 (-283, -33.2)

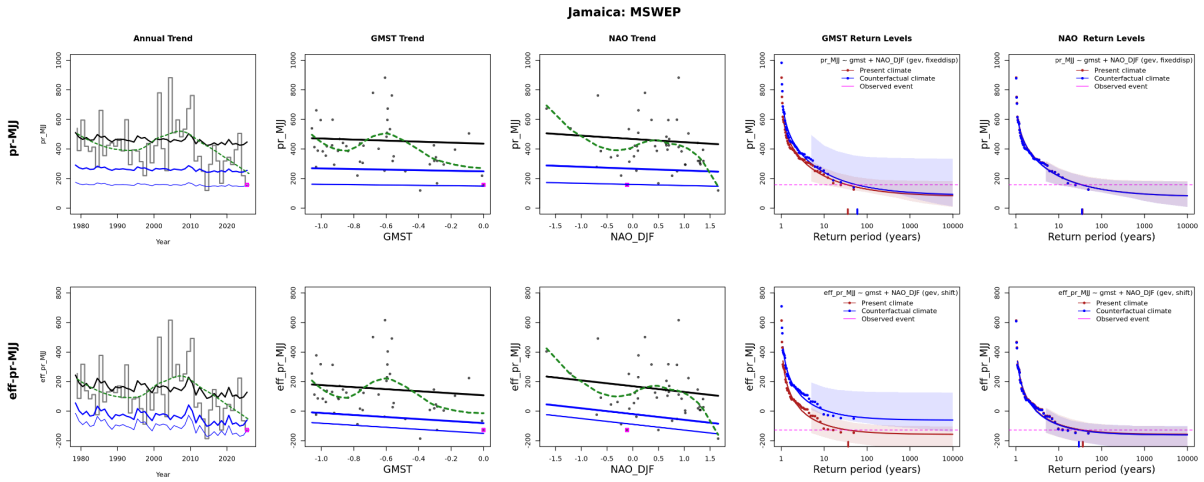


Figure 2.1.2.1*: Jamaica region MSWEP/MSWX reanalysis data, with pr-MJJ on the top row and eff-pr-MJJ on the bottom row, numbered from left to right: 1, annual time series of index. 2, the relationship between the index and 4-year smoothed global mean surface temperatures. 3, the relationship between the index and the DJF NAO. The 2026 event is shown with a pink box; the loess-smoothed trend is shown with the green dashed line and the fitted statistical model that varies with GMST is shown with the black and blue lines, showing the event (black line), and the 1-in-6 (bold blue) and 1-in-40-year (lighter blue) return period event magnitudes. 4, statistical fit of the index to GMST. 5, statistical fit of the model to DJF NAO. The probability curve for the current climate is shown in red, and for the past 1.4°C climate in blue, with the shaded band showing the 95% confidence interval. The magnitude of the studied event is highlighted with a horizontal pink line. Red and blue markers on the return-period axis mark the return period for an event of the 2026 magnitude in the current and past climate respectively. Equivalent plots for CHIRPS/CHIRTS included in the appendix.*

2.1.3 Puerto Rico observed trends

In Puerto Rico, a strong decreasing effect is seen in early wet season precipitation (pr-MJJ) and effective precipitation (eff-pr-MJJ) in MSWEP, though it has not emerged from natural variability as in Jamaica. There is a mixed trend seen in CHIRPS, with an increase in precipitation and a decrease in effective precipitation.

MSWEP finds a decrease in precipitation of -18.7% (95% CI: -48.3% to 8.48%), and in effective precipitation of -26.8 mm (95% CI: -214 mm to 62.1 mm); corresponding to best estimates on the probability ratio of an event this dry of 9.01 and 3.15. CHIRPS finds a decrease in precipitation of 1.91% (95% CI: -32.1% to 13.2%), with this increase substantially smaller than the decrease seen in MSWEP. Accounting for potential evapotranspiration, there is an -7.98 mm (95% CI: -142 mm to 122 mm) decrease in effective precipitation according to CHIRPS.

Table 2.1.3.1: Probability ratio and change in magnitude for May-July precipitation and effective precipitation in the Puerto Rico study region.

	Puerto Rico			
	pr-MJJ		eff-pr-MJJ	
	Probability Ratio	Relative Intensity Delta (%)	Probability Ratio	Absolute Intensity Delta (mm)
CHIRPS	0.650 (0.115, Inf)	1.91 (-32.1, 13.2)	1.28 (0.127, Inf)	-7.98 (-142, 122)
MSWEP	9.01 (0.415, Inf)	-18.7 (-48.3, 8.48)	3.15 (0.265, Inf)	-26.8 (-214, 62.1)

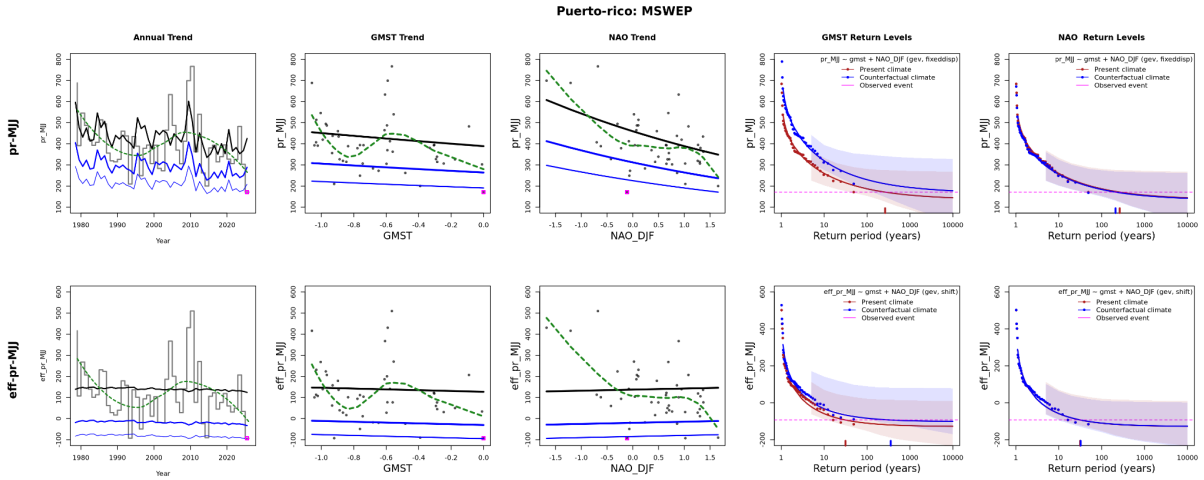


Figure 2.1.3.1*: Puerto Rico region MSWEP/MSWX reanalysis data, with pr-MJJ on the top row and eff-pr-MJJ on the bottom row, numbered from left to right: 1, annual time series of index. 2, the relationship between the index and 4-year smoothed global mean surface temperatures. 3, the relationship between the index and the DJF NAO. The 2026 event is shown with a pink box; the loess-smoothed trend is shown with the green dashed line and the fitted statistical model that varies with GMST is shown with the black and blue lines, showing the event (black line), and the 1-in-6 (bold blue) and 1-in-40-year (lighter blue) return period event magnitudes. 4, statistical fit of the index to GMST. 5, statistical fit of the model to DJF NAO. The probability curve for the current climate is shown in red, and for the past 1.4°C climate in blue, with the shaded band showing the 95% confidence interval. The magnitude of the studied event is highlighted with a horizontal pink line. Red and blue markers on the*

return-period axis mark the return period for an event of the 2026 magnitude in the current and past climate respectively.Equivalent plots for CHIRPS/CHIRTS included in the appendix.

2.1.3.1 Puerto Rico station trends

The precipitation data from eleven individual weather stations across Puerto Rico were collected and analysed to interpret the quality of the reanalysis data, see Fig. 2.1.3.2 for exact locations. The eleven stations represent a random sample of weather stations that met the criteria of sufficient data between 1960 to present.

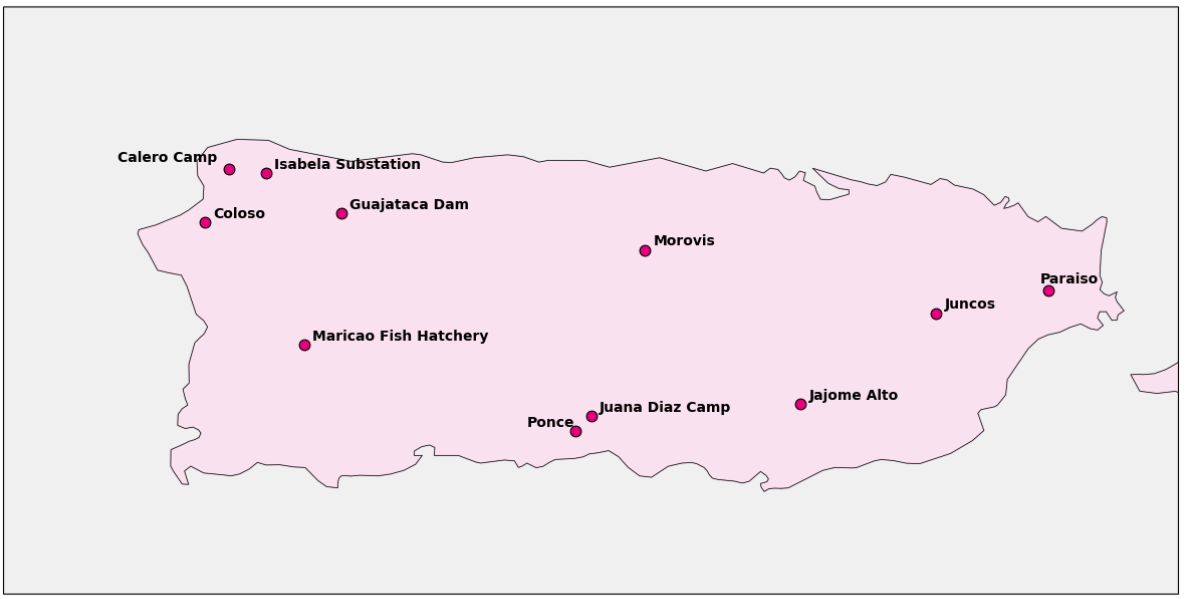


Figure 2.1.3.2*: Map of the Puerto Rican weather stations which were used for station attribution. The results are presented in Table 2.1.3.2.*

To understand how the reanalysis data represent the monthly rainfall data across the study region, first, the data for each station was restricted from January 2025 to present and the monthly average values were calculated. Similarly, the monthly values for both CHIRPS and MSWEP were calculated for the same time period, for the grid box that encompasses the station location. For each station location, the three data sets, observed precipitation station values, CHIRPS and MSWEP, were plotted and compared and can be seen in Fig. 2.1.3.3. There is no real agreement between the three data sets, thus indicating that the reanalysis data is inadequate over the study region. Therefore, results must be treated with caution. In addition, there is a discrepancy between the amount of rainfall that actually fell. Both reanalysis data products over predict the volume of rainfall, with neither reanalysis data product comparatively more accurate than the other.



Figure 2.1.3.3*: Puerto Rico weather station monthly precipitation averages from January 2025 to August 2026 in comparison to CHIRPS and MSWEP data for those point locations. The locations of each station can be seen in Fig. 2.1.3.2.*

Next, attribution analysis was carried out for each of the eleven stations, with data from 1960 to present. The 3-month (MJJ) average rainfall was calculated as in previous sections, and the

results are presented in Table 2.1.3.2. The analysis suggests that the current low rainfall event is not common across any of the stations, with return periods ranging from 4 to 76 years. Probability ratios across all stations range from 0.35 to 3.43, though due to the pointwise nature of station-based analysis the uncertainty margins on these estimates are very wide. Overall, with the exception of three stations, a decrease in the amount of rainfall that fell was found as a result of climate change. Estimates of the decrease range from -0.09% to -29% depending on the geographical location. Three locations, Maricao Fish Hatchery, Morovis and Paraiso show an increase in rainfall in the 3-month period. Nevertheless, all confidence intervals range from negative to positive, showing no emergence from natural variability. Therefore, we must acknowledge the difference between the drying signal as aggregated over the island in observations and models versus at individual locations.

Table 2.1.3.2: Puerto Rico weather stations (data from 1960-present) individually attributed to ascertain local changes in rainfall trends. The locations of each station can be seen in Fig. 2.1.3.2.

	Event Magnitude (mm/day)	**Return Period**	**Probability Ratio**	**Change in Intensity (%)**
Calero Camp	1.77	57.9 (12.3, Inf)	3.43 (0.67, Inf)	-19.4 (-50.0, 10.4)
Coloso	5.86	6.03 (2.95, 22.14)	1.32 (0.31, 5.32)	-4.37 (-21.1, 19.2)
Guajataca Dam	2.47	30.8 (13.3, 183)	1.00 (0.40, 19.0)	-0.09 (-31.7, 48.2)
Isabela Substation	0.06	76.2 (25.2, Inf)	1.27 (0.49, Inf)	-7.44 (-42.5, 44.6)
Jajome Alto	2.18	9.97 (5.22, 36.2)	2.64 (0.70, Inf)	-25.4 (-46.7, 10.9)
Juana Díaz Camp	1.20	4.08 (2.44, 8.48)	1.74 (0.68, 4.52)	-29.0 (-57.1, 24.7)
Juncos	1.45	52.2 (21.2, Inf)	1.77 (0.32, Inf)	-13.7 (-38.3, 19.4)
Maricao Fish Hatchery	3.72	47.8 (13.1, 2970)	0.50 (0.06, 73.9)	12.4 (-22.4, 57.3)
Morovis	1.97	30.4 (9.34, Inf)	0.35 (0.00, Inf)	26.9 (-23.2, 72.4)
Paraiso	2.70	38.6	0.81	4.04

		(13.7, Inf)	(1.86E-06, Inf)	(-35.4, 42.9)
Ponce	0.42	28.4 (11.6, Inf)	2.27 (0.22, Inf)	-23.4 (-61.0, 38.6)

2.1.4 Lesser Antilles observed trends

In the Lesser Antilles, a strong increasing effect is seen in early wet season precipitation (pr-MJJ) in CHIRPS, though this wetting trend disappears when potential evapotranspiration is accounted for. In MSWEP trends are mixed, with a small drying trend observed in precipitation, and a small wetting trend in effective precipitation.

CHIRPS shows an increase in precipitation of +24.5% (95% CI: -24.0% to +35.9%), although in effective precipitation it is only +1.86 mm (95% CI: -12.9 mm to 16.7 mm), corresponding to probability ratio estimates of 0.42 and 0.71 respectively. In MSWEP, a mild decrease in precipitation of -4.16% (95% CI: -28.4% to 43.6%) is seen, with an increase in effective precipitation of 23.6 mm (95% CI: -80.0 mm to 132 mm).

Table 2.1.4.1: Probability ratio and change in magnitude for May-July precipitation and effective precipitation in the Lesser Antilles study region.

	Lesser Antilles			
	pr-MJJ		eff-pr-MJJ	
	Probability Ratio	Relative Intensity Delta (%)	Probability Ratio	Absolute Intensity Delta (mm)
CHIRPS	0.419 (0.329, 13.2)	24.5 (-24.0, 35.9)	0.706 (0.245, Inf)	1.86 (-12.9, 16.7)
MSWEP	1.24 (0.297, Inf)	-4.16 (-28.4, 43.6)	0.665 (0.263, Inf)	23.6 (-80.0, 132)

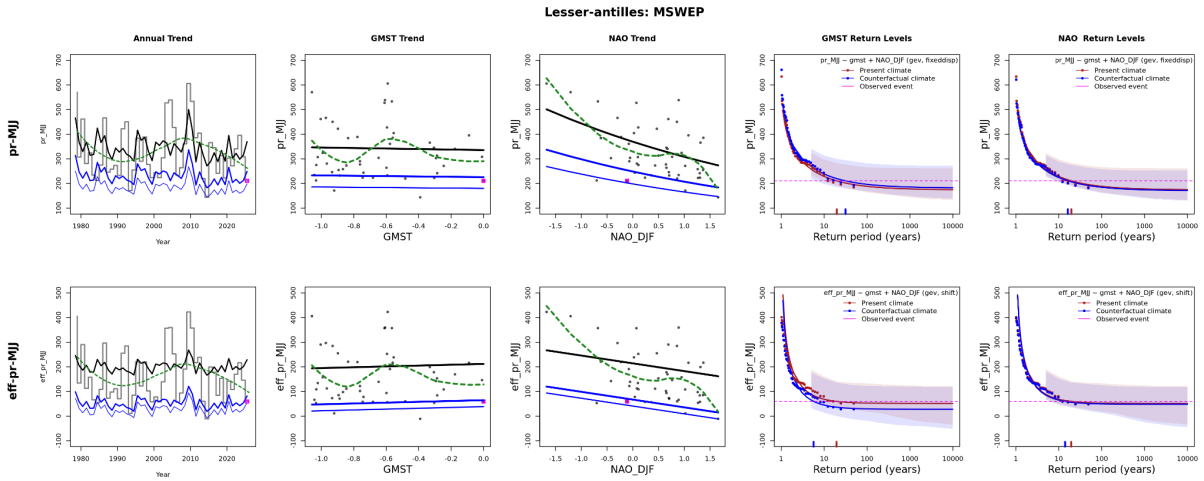


Figure 2.1.4.1*: Lesser Antilles region MSWEP/MSWX reanalysis data, with pr-MJJ on the top row and eff-pr-MJJ on the bottom row, numbered from left to right: 1, annual time series of index. 2, the relationship between the index and 4-year smoothed global mean surface temperatures. 3, the relationship between the index and the DJF NAO. The 2026 event is shown with a pink box; the loess-smoothed trend is shown with the green dashed line and the fitted statistical model that varies with GMST is shown with the black and blue lines, showing the event (black line), and the 1-in-6 (bold blue) and 1-in-40-year (lighter blue) return period event magnitudes. 4, statistical fit of the index to GMST. 5, statistical fit of the model to DJF NAO. The probability curve for the current climate is shown in red, and for the past 1.4°C climate in blue, with the shaded band showing the 95% confidence interval. The magnitude of the studied event is highlighted with a horizontal pink line. Red and blue markers on the return-period axis mark the return period for an event of the 2026 magnitude in the current and past climate respectively. Equivalent plots for CHIRPS/CHIRTS included in the appendix.*

2.1.5 Observed trends in seasonal mean temperature

Tables 2.1.5.1-2.1.5.3 (Figures summarise the trend-fitting for the seasonal (MJJ) average temperature for Puerto Rico, Jamaica and the lesser Antilles regions based on the CHIRTS and MSWX datasets. The temperatures observed this year are not unprecedented in any of the study regions, according to these datasets. The return periods are less than two years for the observed temperatures in today's climate for Puerto Rico and the lesser Antilles, and around ~3 years for Jamaica, suggesting that high seasonal temperatures are routine occurrences in today's climate. However, the trends from fitting a non-stationary Gaussian distribution that scales with GMST to the time series of MJJ average temperatures suggest strong warming trends in all three regions, with ~1.2°C, ~1.6°C and ~1.1°C increases in the average temperatures observed in 2026 over Puerto Rico, Jamaica and the Lesser Antilles regions respectively, associated with the 1.4°C warming since pre-industrial times. The PRs are also very high with best estimates greater than 100 across all datasets and all regions, suggesting that the MJJ season in all three regions have been made significantly warmer due to climate

change. The fact that temperatures show such a strong observed trend compared to potential evapotranspiration (which strongly responds to temperature) is likely a result of SST increases which drive higher humidity which in turn brings down evaporative demand.

Table 2.1.5.1*: Event magnitudes, return periods in today's climate, Probability ratio and change in magnitude for May-July seasonal temperature in the Puerto Rico study region.*

dataset	event_magnitude	return_period	PR	dI_abs
CHIRTS	29.34	1.20 (1.02 to 1.99)	1850 (82.52 to >1m)	1.26 (0.75 to 1.84)
MSWX	26.90	1.97 (1.19 to 5.81)	3940 (132.00 to >1m)	1.15 (0.63 to 1.69)

Table 2.1.5.2*: Event magnitudes, return periods in today's climate, Probability ratio and change in magnitude for May-July seasonal temperature in the Jamaica study region.*

dataset	event_magnitude	return_period	PR	dI_abs
CHIRTS	27.48	2.19 (1.36 to 6.32)	>1m (>1m to >1m)	1.68 (1.27 to 2.06)
MSWX	27.30	3.95 (2.15 to 15.53)	>1m (>1m to >1m)	1.78 (1.37 to 2.13)

Table 2.1.5.3*: Event magnitudes, return periods in today's climate, Probability ratio and change in magnitude for May-July seasonal temperature in the Lesser Antilles study region.*

dataset	event_magnitude	return_period	PR	dI_abs
CHIRTS	30.5	1.31 (1.04 to 2.39)	292 (22.9 to 22500)	1.15 (0.61 to 1.73)
MSWX	27.0	1.61 (1.14 to 3.55)	498.01 (32.3 to 29500)	0.99 (0.54 to 1.50)

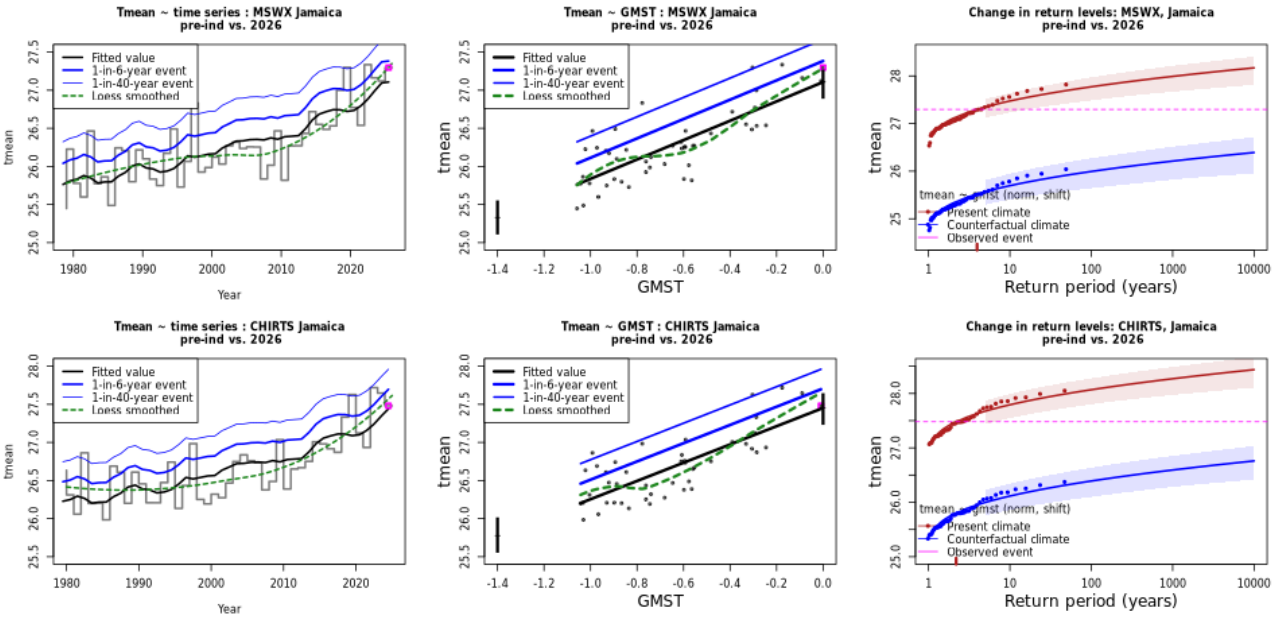


Figure 2.1.5.1*: (a) MJJ seasonal mean temperature time series over Jamaica, (b) same as (a) but plotted against GMST. (c) Return period curves from fitting a non-stationary Gaussian distribution that shifts with gmst to the seasonal mean temperatures. The 2026 event is shown with a pink box; the loess-smoothed trend is shown with the green dashed line and the fitted statistical model that varies with GMST is shown with the black and blue lines, showing the event (black line), and the 1-in-6 (bold blue) and 1-in-40-year (lighter blue) return period event magnitudes. 4, statistical fit of the index to GMST. 5, statistical fit of the model to DJF NAO. The probability curve for the current climate is shown in red, and for the past 1.4°C climate in blue, with the shaded band showing the 95% confidence interval. The magnitude of the studied event is highlighted with a horizontal pink line. Red and blue markers on the return-period axis mark the return period for an event of the 2026 magnitude in the current and past climate respectively.Equivalent plots for CHIRPS/CHIRTS included in the appendix.*

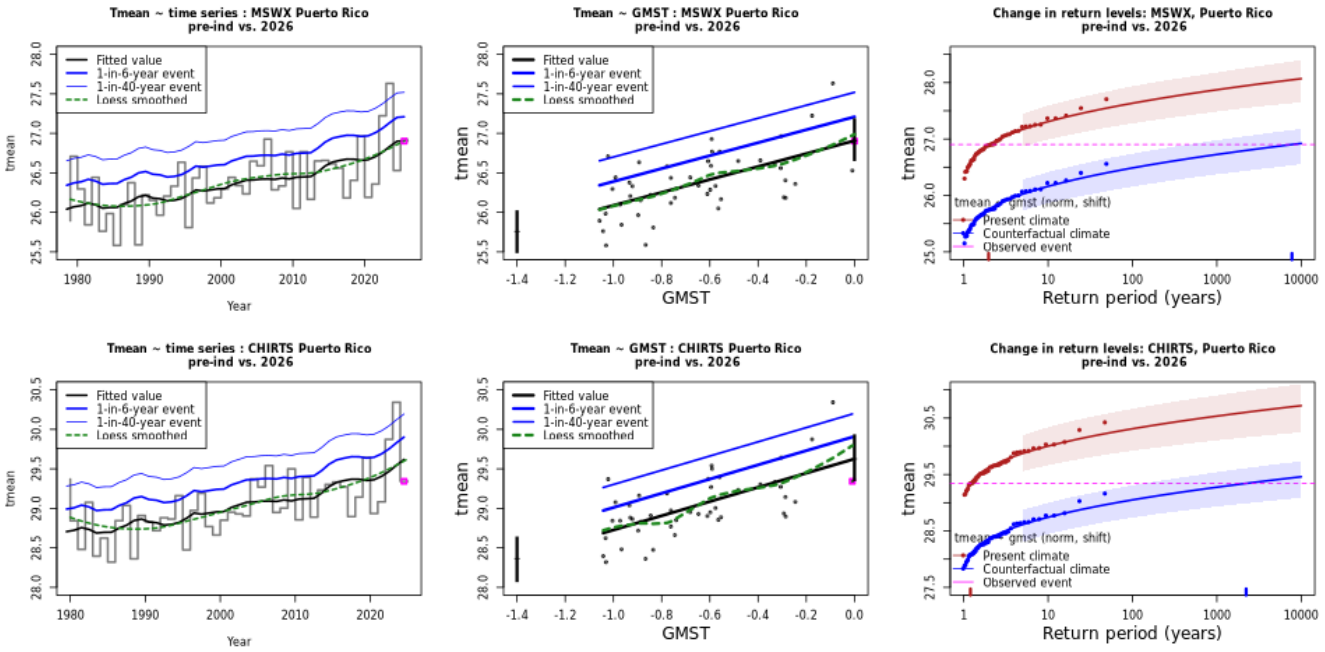


Figure 2.1.5.2*: same as Figure 2.1.5.1 for Puerto Rico*

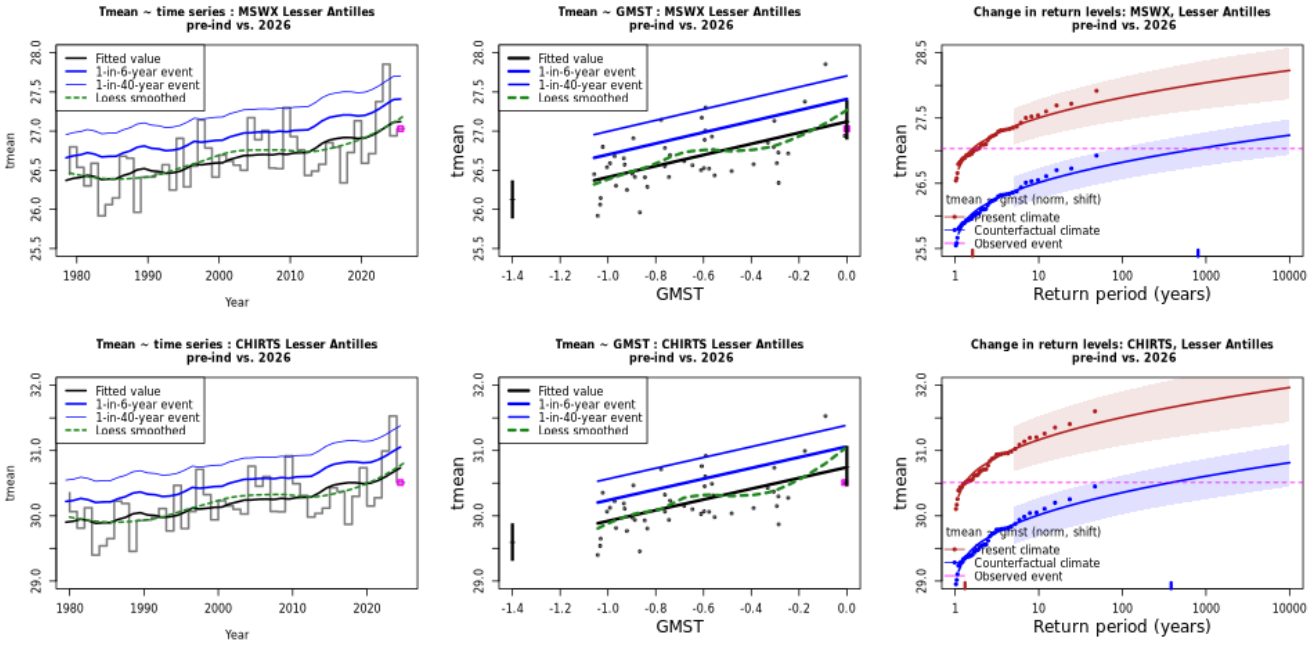


Figure 2.1.5.3*: same as Figure 2.1.5.1 for the Lesser Antilles.*

2.1.6 Compound event attribution for precipitation and PET

The coloured areas in Fig. 2.1.6.1 show the US Drought Monitor drought classifications based on SPEI, standardised with respect to the 1991–2020 climatology, in which SPEI values greater than -0.5 are 'normal or wet conditions'; -0.5 to -0.8 are abnormally dry (D0); -0.8 to -1.3 are moderate drought (D1); -1.3 to -1.6 are severe drought (D2); -1.6 to -2 are

extreme drought (D3); and values less than -2 are exceptional drought (D4). For all study regions, the classifications are derived from SPEI-3, calculated using accumulated precipitation and potential evapotranspiration (PET) over the three-month period from May to July, using the Hargreaves scheme for PET.

The solid lines are contours representing combinations of precipitation and PET with equal probability of occurring in the 2026 climate, based on the joint distribution of these variables (see WWA 2023 East Africa Drought for details). The contours are labelled with their corresponding return periods, and the magenta dot marks the precipitation and PET observed in 2026. The dotted lines show the corresponding contours for a climate that is 1.4°C cooler, while the turquoise dot indicates an event in that cooler climate with the same rarity as the 2026 event.

In all study regions, the shift in the joint distribution, and hence the increase in drought severity is seen to be driven primarily by decreases in the seasonal rainfall, rather than changes in PET. The combinations of observed precipitation and PET combination during the three month long drought in 2026 have return periods of approximately 15, 20 and 5 years in Jamaica, Puerto Rico and the Lesser Antilles region respectively, highlighting that the drought conditions over Jamaica and Puerto Rico this year is unusual, as suggested by the high return periods. These conditions are classified as an extreme drought (D2) in both Puerto Rico and Jamaica in today's climate, whereas over the Lesser Antilles, the conditions this year seemingly correspond to a milder 'moderate' (D1) drought conditions. By contrast, the precipitation and PET combinations of equivalent rarity in a climate 1.4°C cooler would have resulted in less intense drought conditions, classified as a severe drought (D2) in Puerto Rico and moderate drought in Jamaica and the Lesser Antilles, following the same 1991-2020 baseline. It can be seen from Figure 2.1.6.1 that, although changes in PET also contribute to shifts in the joint distributions in all three regions, the increase in the severity of the 2026 drought is primarily associated with reductions in seasonal rainfall. In a climate 1.4°C cooler, the same low precipitation amounts would need to be accompanied by higher PET, to yield droughts of similar rarity to those observed in today's climate. However, because the decreases in rainfall have been more pronounced between the 2026 and the 1.4°C cooler climates (as compared to the much smaller changes in PET), droughts have become more severe in today's climate. In other words, for a given PET, droughts of any given rarity are associated with lower precipitation amounts in today's climate.

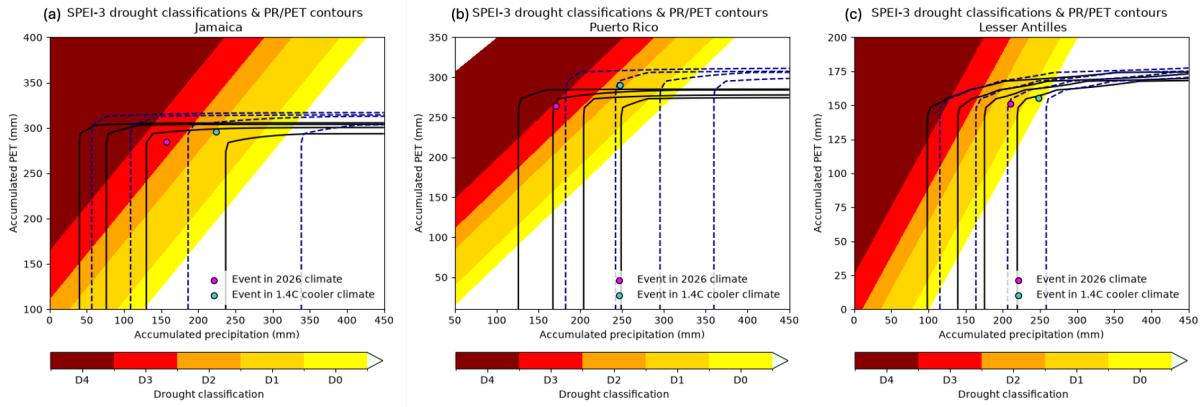


Figure 2.1.6.1*: (a) US Drought Monitor drought classifications based on SPEI, standardised with respect to the 1991–2020 climatology for the 3- month long (MMJ) drought in Jamaica. The solid contours indicate return periods under the joint distribution in the current climate, while the dashed contours indicate the same return periods in a 1.4°C cooler climate. The shaded contours represent different levels of drought severity (D0-D4). The magenta point indicates the accumulated precipitation and PET observed in 2026; the turquoise point shows an event of equivalent rarity in a 1.4°C cooler climate. (b) same as (a) for Puerto Rico. (c) same as (a) for the Lesser Antilles. [Source MSWEP/MSWX]*

3 Attribution of trends

3.1 Evaluation of climate models

In the subsections below we show the results of the model evaluation for each location. The climate models are evaluated against the observations in their ability to capture:

1. Seasonal cycles: For this, we qualitatively compare the seasonal cycles based on model outputs against observations-based cycles. We discard the models that exhibit ill-defined peaks in their seasonal cycles. We also discard the model if the rainy season onset/termination varies significantly from the observations.
2. Spatial patterns: Models that do not match the observations in terms of the large-scale precipitation patterns are excluded.
3. Parameters of the fitted statistical models. We discard the model if the model and observation parameters ranges do not overlap.

In total, we evaluated 15 CORDEX and 13 HighResMIP precipitation models using these three criteria (see Appendix A1.2 for model descriptions). For the evaluation of seasonal cycles and spatial patterns, the three subregions were considered together. This was appropriate because they have broadly similar climatological characteristics and also reduced the risk of excluding models simply because they do not adequately resolve the small land areas of the Lesser Antilles.

The models are labelled as ‘good ’, ’ reasonable ’, or ‘bad’ based on their performance in terms of the three criteria discussed above. A model is given an overall rating of ‘good’ if it is rated ‘good’ for all three characteristics. If there is at least one ‘reasonable’, then its overall rating will be ‘reasonable ’, and ‘bad’ if there is at least one ‘bad’. We used all models with the label 'good’ as well as the models with one or two labels 'reasonable'. Overall, both CORDEX and HighResMIP models showed satisfactory performance, although the number of models passing the evaluation varied across the three study regions. For Puerto Rico, 13 CORDEX and 6 HighResMIP models passed the evaluation; for the Lesser Antilles, 12 CORDEX and 9 HighResMIP models passed; and for Jamaica, 9 CORDEX and 8 HighResMIP models passed. Tables of the model evaluation results can be found in Appendix A2.

3.2 Synthesis of results

For the event definitions described above we evaluate the influence of anthropogenic climate change and the DJF NAO on the events by calculating the probability ratio as well as the change in intensity using observations and climate models. Models which do not pass the evaluation described above are excluded from the analysis. The aim is to synthesise results from models that pass the evaluation along with the observations-based products, to give an overarching attribution statement. Tables of the results of this model fitting can be found in Appendix A3.

Figures in this section show the changes in probability and intensity for the observations (blue) and models (red). Before combining them into a synthesised assessment, first, a representation error is added (in quadrature) to the observations, to account for the difference between observations-based datasets that cannot be explained by natural variability. This is shown in these figures as white boxes around the light blue bars. The dark blue bar shows the average over the observation-based products. Next,] [a term to account for intermodel spread is added (in quadrature) to the natural variability of the models. This is shown in the figures as white boxes around the light red bars. The dark red bar shows the model average, consisting of a weighted mean using the (uncorrelated) uncertainties due to natural variability plus the term representing intermodel spread (i.e., the inverse square of the white bars).

Observation-based products and models are combined into a single result in two ways. Firstly, we neglect common model uncertainties beyond the intermodel spread that is depicted by the model average, and compute the weighted average of models (dark red bar) and observations (dark blue bar): this is indicated by the magenta bar. As, due to common model uncertainties, model uncertainty can be larger than the intermodel spread, secondly, we also show the more conservative estimate of an unweighted, direct average of observations (dark blue bar) and models (dark red bar) contributing 50% each, indicated by the white box around the magenta bar in the synthesis figures.

3.2.1 Jamaica

In Jamaica, models and observations both show a drying response to warming – for both meteorological and agricultural drought. For precipitation only (pr-MJJ), we find good

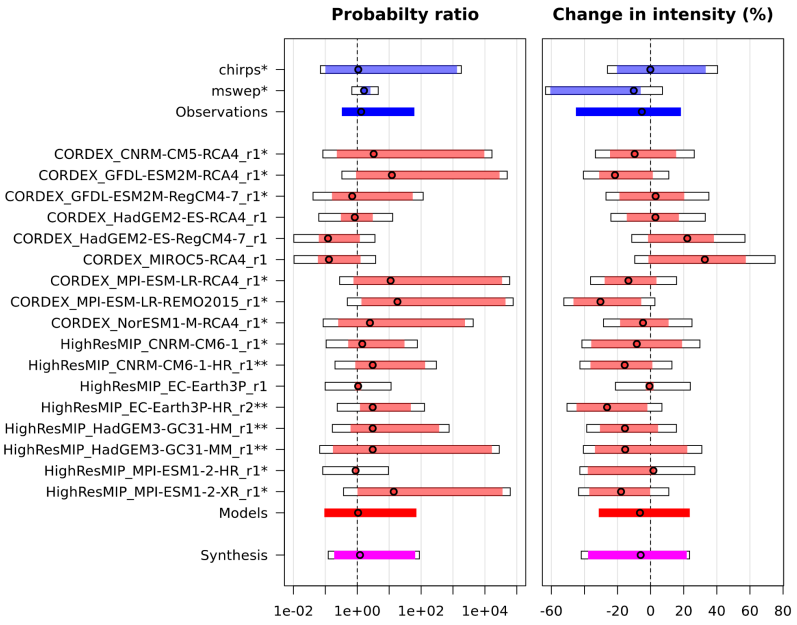
agreement – with central estimates of the climate change driven decrease in rainfall of 5.3% in the observations, 6.4% in the observations, and 6.0% according to the synthesis of both. Climate model projections show a decrease of 9.9% for a further +1.4°C global warming. For effective precipitation, there is a much stronger decrease in early wet season potential moisture in observations (48 mm) than in models (15 mm), though both agree on an increase in the likelihood of dry conditions – with a central estimate of a +38% (95% CI : -55% to +1120%) increase in likelihood (converted to percentage change from absolute change) of this event due to human caused climate change.

Of potential importance is that the strength of this trend is stronger in future projections compared to historic climate change. The climate models show good agreement with observations in the precipitation trend, though show a reduced magnitude of effect when accounting for potential evapotranspiration. Uncertainty estimates are nonetheless very wide, partially due to the short record in the case of the observations. In addition, it cannot be ruled out that models and reanalysis data perform poorly – given the evaluation in section 2.1.3.1 over Puerto Rico – and shortcomings of climate models in representing observed patterns in the region (Vichot–Llano et al., 2020).

Combining lines of evidence from the synthesis of results of the past climate, we find that there likely is a climate change driven decrease in early wet season rainfall and effective precipitation over Jamaica – exacerbating the drought conditions seen in August, 2026.

Table 3.2.1.1*: Summary of results for pr-MJJ and eff-pr-MJJ over Jamaica, presented in Figs 3.2.1.1 and 3.2.1.2: changes due to GMST include past-present changes and present-future changes for the NAO DJF state of 2025/26. Statistically significant increases (decreases) in probability and intensity are highlighted in darker blue (orange), while non-significant increases are highlighted in light blue (orange). Statistically significant changes are also highlighted in bold font.*

Data	Period	Precipitation		Effective Precipitation	
		Probability ratio (95% CI)	Intensity change (%) (95% CI)	Probability ratio (95% CI)	Intensity change (mm) (95% CI)
Observations	Past - Present	1.33 (0.330, 61.7)	-5.31 (-45.1, 18.3)	59.6 (10^{-4}, >1m)	-48.4 (-232, 113)
Models		1.06 (0.093, 71.3)	-6.43 (-31.3, 23.7)	1.35 (0.734, 7.40)	-15.2 (-60.3, 27.6)
Synthesis		1.22 (0.190, 65.4)	-6.02 (-37.8, 21.8)	1.38 (0.453, 12.2)	-17.2 (-80.1, 40.3)
Models only	Present -Future	2.12 (0.716, 5.70)	-9.94 (-27.8, 9.19)	2.88 (0.672, 8.49)	-25.8 (-59.0, 6.83)



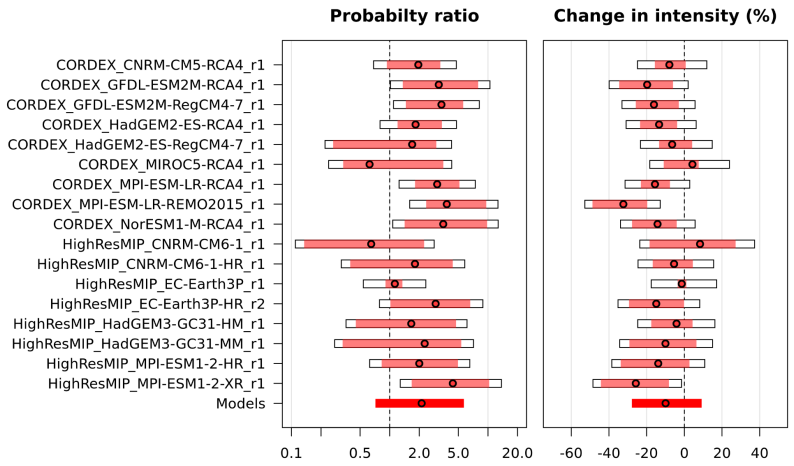
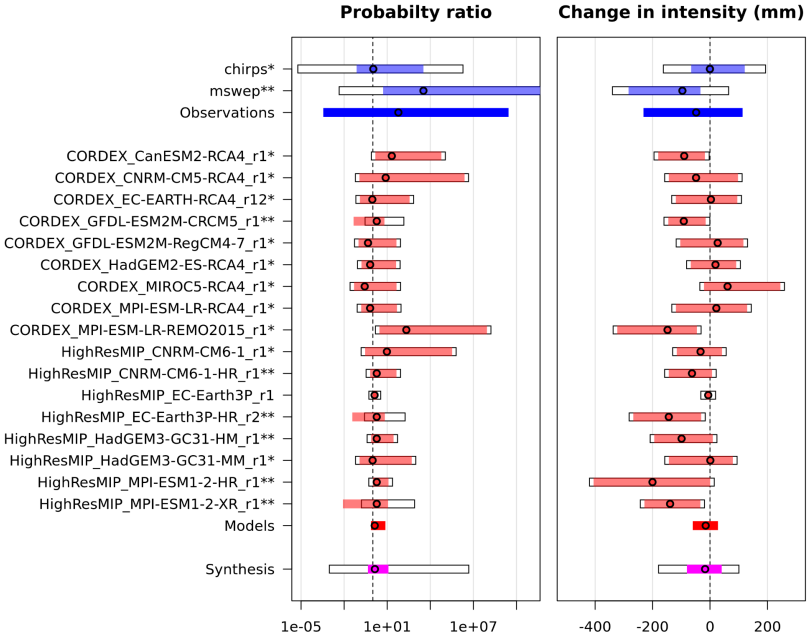


Figure 3.2.1.1*: Above: synthesised changes in (left) likelihood and (right) changes in intensity of Jamaica pr-MJJ when comparing the 2026 climate and a 1.4°C cooler climate representing the preindustrial past. Observation-based datasets are shown in blue, climate models are shown in red, and the synthesis is shown in magenta. Below: change in probability (left) and intensity (right) for pr-MJJ in the study region between the current climate and a future, 1.4°C warmer climate.*



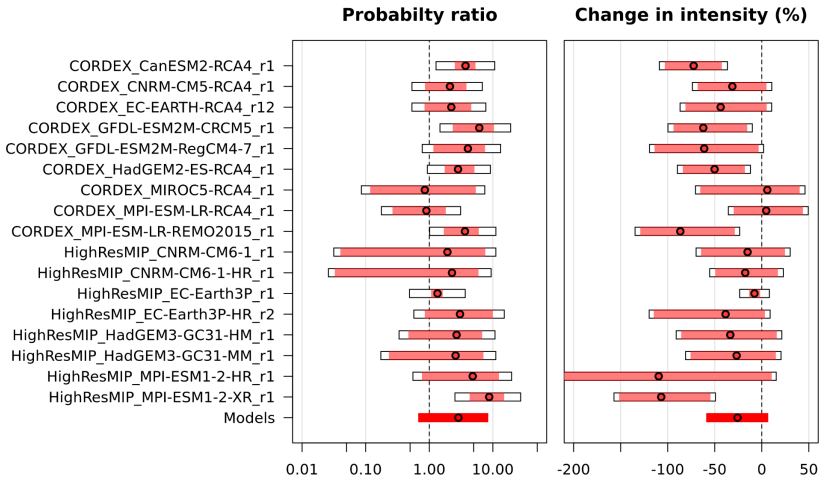


Figure 3.2.1.2*: Above: synthesised changes in (left) likelihood and (right) changes in intensity of Jamaica eff-pr-MJJ when comparing the 2026 climate and a 1.4°C cooler climate representing the preindustrial past. Observation-based datasets are shown in blue, climate models are shown in red, and the synthesis is shown in magenta. Below: change in probability (left) and intensity (right) for eff-pr-MJJ in the study region between the current climate and a future, 1.4°C warmer climate.*

3.2.2 Puerto Rico

In Puerto Rico, models and observations also both show a drying response to warming – for both precipitation and effective precipitation.

For both pr-MJJ and eff-pr-MJJ, there is good agreement in the magnitude of the response. For precipitation, observations show a -9.0% decrease, models -8.7% and the synthesis of models and observations -8.7% (95% CI: -33.5% to 17.5%). For effective precipitation, observations find a slightly larger -17 mm decrease, with models (-11 mm) and the synthesis (-12 mm, with a 95% CI of -77 mm to 39 mm) both showing a similar effect. Climate model projections are stronger than the historic signal for both drought metrics, with the 95% confidence interval emergent from natural variability when potential evapotranspiration is accounted for (e ff-pr-MJJ) -30 mm (-59 mm to -3.2 mm).

This increase in modelled trend with future warming is similar to that seen over Jamaica, and uncertainty estimates are again wide due to high natural variability. Additionally, point-wise comparisons to reanalysis and station data over Puerto Rico are poor at monthly accumulations in recent years (Section 2.1.3.1). Nonetheless, these results indicate that there is likely a substantial drying trend in Puerto Rico in the early wet season which made 2026's drought more likely. Increases in MJJ dry days and decreased precipitation are expected to continue into at least the mid 21st century (Ramseyer et al. 2019). Van Beusekom et al. (2017) showed that cloud levels in the dry season are consistently as low or lower than in the wet seasons at a low-elevation tropical mountain cloud forest (TMCF) in Puerto Rico under

the current climate regime, indicating that the TMCF ecosystem may be more vulnerable to wet-season drought periods.

Table 3.2.2.1*: Summary of results for pr-MJJ and eff-pr-MJJ over Puerto Rico, presented in Figs 3.2.2.1 and 3.2.2.2: changes due to GMST include past-present changes and present-future changes for the NAO DJF state of 2025/26. Statistically significant increases (decreases) in probability and intensity are highlighted in darker blue (orange), while non-significant increases are highlighted in light blue (orange). Statistically significant changes are also highlighted in bold font.*

Data	Period	Precipitation		Effective Precipitation	
		Probability ratio (95% CI)	Intensity change (%) (95% CI)	Probability ratio (95% CI)	**Intensity change (mm) (95% CI)**
Observations	Past - Present	2.42 (0.031, 7790)	-8.99 (-46.5, 31.8)	2.01 (0.136, 2910)	-17.4 (-180, 94.9)
Models		1.21 (0.134, 69.7)	-8.65 (-27.7, 13.1)	1.27 (0.698, 5.62)	-11.5 (-56.9, 28.9)
Synthesis		1.39 (0.086, 234)	-8.72 (-33.5, 17.5)	1.29 (0.579, 10.4)	-12.0 (-77.0, 39.1)
Models only	Present -Future	1.93 (0.700, 5.23)	-11.3 (-32.6, 12.5)	2.49 (0.431, 9.14)	**-29.6 (-58.9, -3.18)**

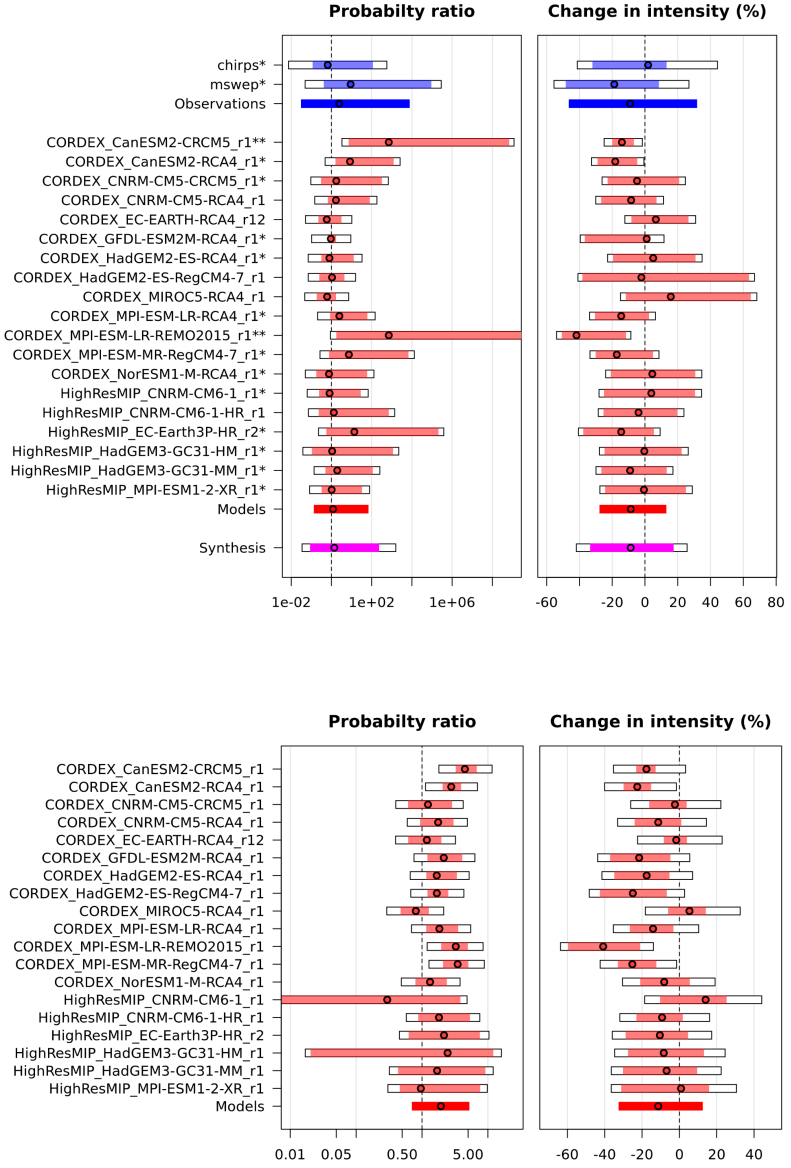


Figure 3.2.2.1*: Above: synthesised changes in (left) likelihood and (right) changes in intensity of Puerto Rico pr-MJJ when comparing the 2026 climate and a 1.4°C cooler climate representing the preindustrial past. Observation-based datasets are shown in blue, climate models are shown in red, and the synthesis is shown in magenta. Below: change in probability (left) and intensity (right) for pr-MJJ in the study region between the current climate and a future, 1.4°C warmer climate.*

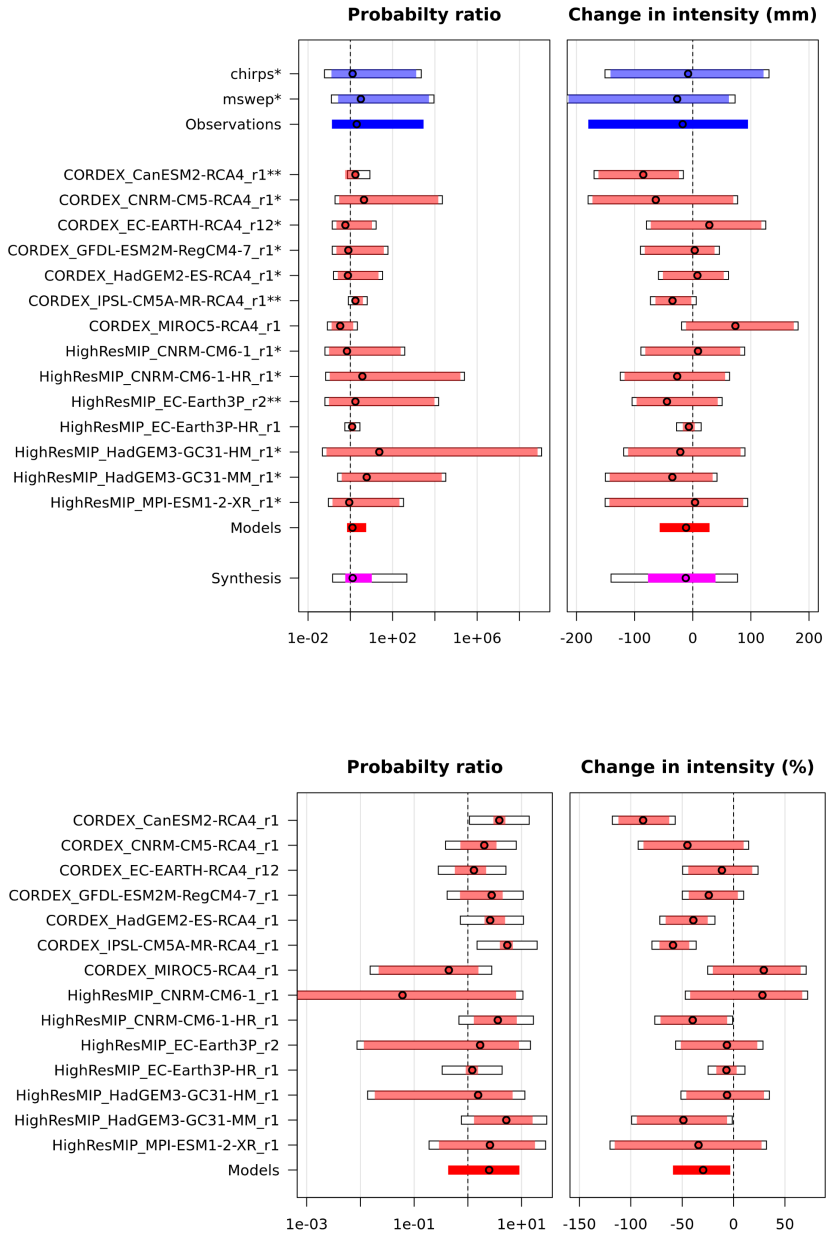


Figure 3.2.2.2*: Above: synthesised changes in (left) likelihood and (right) changes in intensity of Puerto Rico eff-pr-MJJ when comparing the 2026 climate and a 1.4°C cooler climate representing the preindustrial past. Observation-based datasets are shown in blue, climate models are shown in red, and the synthesis is shown in magenta. Below: change in probability (left) and intensity (right) for eff-pr-MJJ in the study region between the current climate and a future, 1.4°C warmer climate.*

3.2.3 Lesser Antilles

Over the Lesser Antilles, observations differ with climate models on the trend in May-July moisture, with observations showing a wetting effect, and climate models a drying one.

For precipitation only, pr-MJJ, observations show an increase of +9.3% (95% CI: -36% to 69%) due to climate change, whilst climate models show a decrease of -7.8% (95% CI: -32% to 19%). Similarly, effective precipitation shows an observed increase of 13 mm (-54 mm to 81 mm) and models a decrease of -23 mm (-91 mm to 42 mm). Unlike for the Puerto Rico and Jamaica regions, the projected future trend is of a similar trend to the historic effect in climate models.

For some variables and regions, a difference in sign of trend between reanalysis based observations and climate model data, would indicate that climate models are not adequately representing key processes. It is established that climate models perform poorly over small islands (Evans et al., 2024), however it is equally possible that the gridded datasets are incorrect – with performance generally worse over the island chain (Centella-Artola et al., 2020). Conclusions are therefore difficult to draw, but further development of precipitation products and climate models targeted at better representing precipitation and temperature over small islands would be helpful in monitoring and projecting drought severity.

Table 3.2.3.1*: Summary of results for pr-MJJ and eff-pr-MJJ over the Lesser Antilles, presented in Figs 3.2.3.1 and 3.2.3.2: changes due to GMST include past-present changes and present-future changes for the NAO DJF state of 2025/26. Statistically significant increases (decreases) in probability and intensity are highlighted in darker blue (orange), while non-significant increases are highlighted in light blue (orange). Statistically significant changes are also highlighted in bold font.*

Data	Period	Precipitation		Effective Precipitation	
		Probability ratio (95% CI)	Intensity change (%) (95% CI)	Probability ratio (95% CI)	Intensity change (mm) (95% CI)
Observations	Past - Present	0.72 (0.129, 46.0)	9.26 (-36.0, 69.4)	0.69 (0.253, 13.4)	12.7 (-53.7, 81.4)
Models		1.09 (0.434, 7.44)	-7.75 (-31.6, 19.3)	1.46 (0.180, 71.3)	-23.1 (-91.4, 41.5)
Synthesis		1.01 (0.330, 12.3)	-3.82 (-33.7, 31.3)	0.864 (0.208, 23.0)	-5.50 (-72.8, 61.2)
Models only	Present -Future	1.40 (0.681, 2.84)	-9.89 (-37.9, 24.1)	1.57 (0.801, 2.95)	-25.2 (-57.2, 1.34)

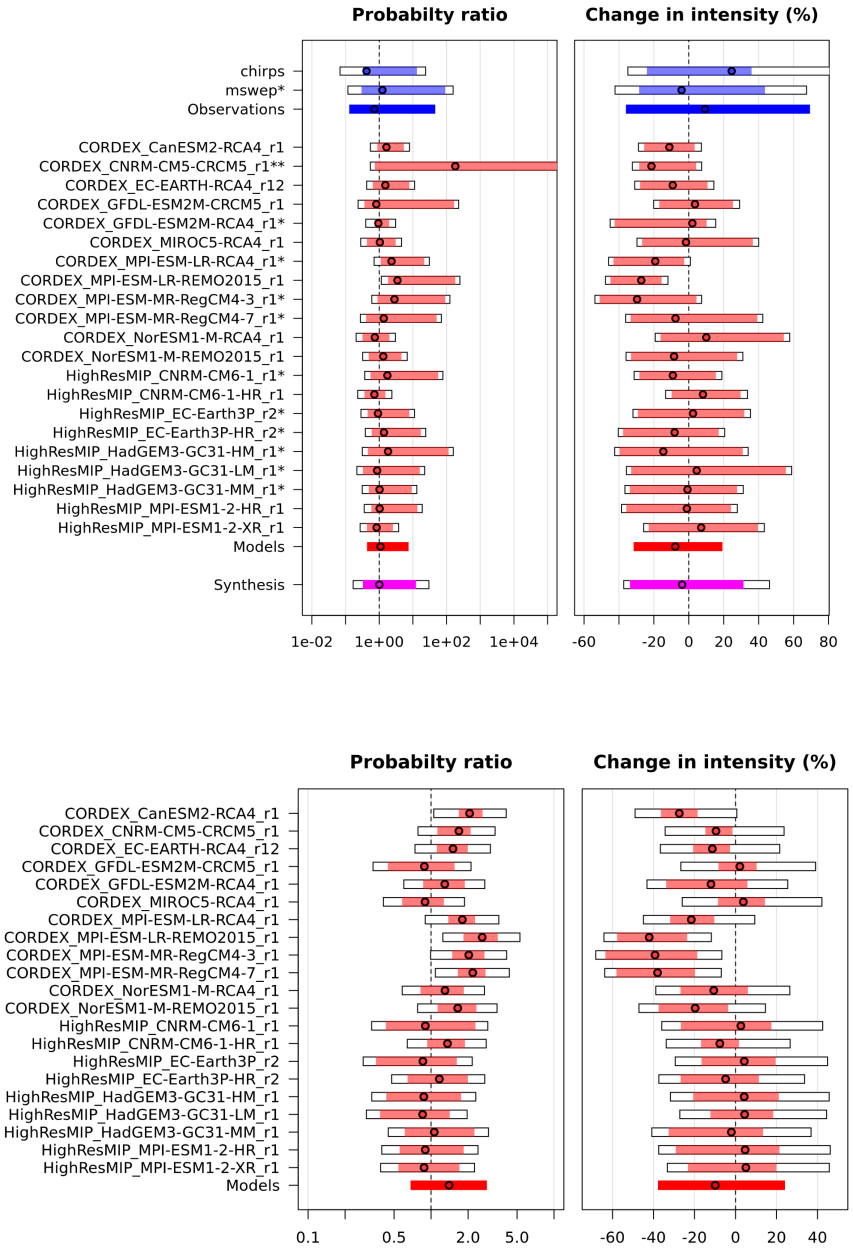


Figure 3.2.3.1*: Above: synthesised changes in (left) likelihood and (right) changes in intensity of the Lesser Antilles pr-MJJ when comparing the 2026 climate and a 1.4°C cooler climate representing the preindustrial past. Observation-based datasets are shown in blue, climate models are shown in red, and the synthesis is shown in magenta. Below: change in probability (left) and intensity (right) for pr-MJJ in the study region between the current climate and a future, 1.4°C warmer climate.*

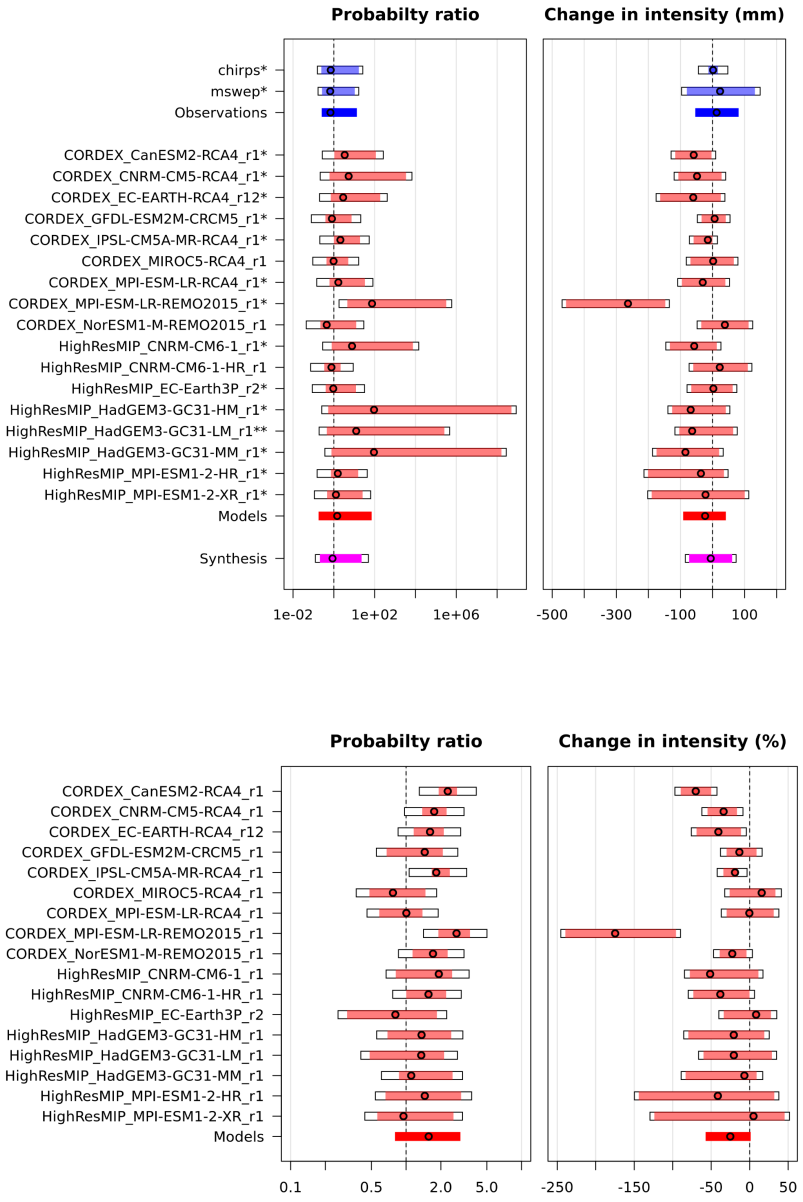


Figure 3.2.3.2*: Above: synthesised changes in (left) likelihood and (right) changes in intensity of the Lesser Antilles eff-pr-MJJ when comparing the 2026 climate and a 1.4°C cooler climate representing the preindustrial past. Observation-based datasets are shown in blue, climate models are shown in red, and the synthesis is shown in magenta. Below: change in probability (left) and intensity (right) for eff-pr-MJJ in the study region between the current climate and a future, 1.4°C warmer climate.*

3.3 Summary of hazard findings

Jamaica and Puerto Rico both show consistent decreases in May-July moisture, across both meteorological and ecological drought. Observations give central estimates of a -5.3% and -9.0% decrease in precipitation, respectively. In effective precipitation there is a -48 mm in Jamaica and -17 mm decrease in Puerto Rico, which are quite small changes for seasonal

rainfall – especially for Puerto Rico. This is because whilst observed seasonal temperatures are very strongly increasing (Section 2.1.5), PET has remained very similar over the southern Caribbean region and with an observed decrease over Puerto Rico. In the Hargreaves scheme, humidity and cloud cover are approximated through the diurnal temperature range – meaning that despite the increase in temperatures, higher cloud cover and humidity are suppressing a rise in PET.

Climate models also represent these decreasing trends for Jamaica and Puerto Rico. In precipitation, central estimates were -6.4% for Jamaica and -8.6% for Puerto Rico rainfall totals due to historic climate change. Unusually, these trends were projected to substantially increase with an equal amount (+1.4°C) of future warming, totalling 9.9% and 11% respectively. Similar effects were also observed for effective precipitation. Synthesis trends closely match those seen in models..

The Lesser Antilles show highly uncertain trends, both in terms of confidence intervals (due to high variability in the studied indices over such small islands) and in disagreement between models and observations – with observations finding a weak wetting trend and models a weak drying one.

4 Vulnerability and exposure

The insular Caribbean comprises three main island groups: the Lucayan Archipelago, the Greater Antilles, and the Lesser Antilles. The affected territories range from upper-middle-income economies (Jamaica, Saint Lucia, St Vincent and the Grenadines, Grenada) to high-income economies (Bermuda, Puerto Rico, St Kitts and Nevis, U.S. Virgin Islands). Five qualify as Small Island Developing States (SIDS) (UN, nd; World Bank, 2025). This region experiences hydrometeorological and climate hazards, including severe droughts, tropical cyclones, extreme wave events, and sea level changes (Hofman et al., 2021). Repeated exposure to these hazards can erode infrastructure, damage water and agricultural systems, degrade ecosystems, and strain household and institutional coping capacity, increasing vulnerability to subsequent extreme events, and in turn, creating cascading and compounding risks. For example, Hurricanes Irma and Maria in 2017, and Melissa in 2025, caused extensive damage to Puerto Rico and Jamaica's utility and agricultural systems, cutting hundreds of thousands of people from centralized water systems for months (Ruiz-Aviles et al., 2022; McGinley et al., 2022; Bello et al., 2026).

This chapter summarises vulnerability, exposure, and coping capacity to drought across Puerto Rico, Jamaica, and parts of the Lesser Antilles. Several key areas will be discussed, including water management practices, livelihoods and food security, and drought risk management.

4.1 Historic impacts of droughts in the Caribbean

The Caribbean region is home to seven of the world's top 36 water-stressed countries, including Antigua and Barbuda, Barbados, as well as St. Kitts and Nevis, which are characterized by water scarcity with less than 1,000 m³ of freshwater resources per capita (FAO, 2016). Across these highly water-limited islands, drought often develops when rainfall deficits coincide with rising temperature and elevated evaporation rates.

The Caribbean experiences intense dry seasons, particularly in years with El Niño events (Giannini et al., 2001; Herrera and Ault, 2017). The Lesser Antilles have experienced more intense, widespread and frequent drought events than the Greater Antilles between 1950 and 2017 (Herrera and Ault, 2017; de Sousa Moraes, 2021). A severe drought during the 2009-2010 season highlighted these issues, exposing the vulnerability of various social groups and sectors (Peters, 2015). This includes farmers, especially smallholders, along with the poor, children, rural and indigenous communities, downstream users, and the tourism industry that is vital to the economy (FAO, 2016).

The Pan-Caribbean drought of 2013-2016 was the most severe since 1950, impacting over 43 million inhabitants within the region, with the 2015-2016 El Niño contributing to precipitation deficits and anthropogenic warming further intensifying its severity through increased evaporative demand (Herrera et al., 2018; Álvarez-Berríos et al., 2018). An assessment conducted by Puerto Rico's Planning Board estimated economic damages amounting to $22.7 million, after accounting for income received by farmers. Of this total, $13.8 million was attributed to the agricultural sector; $3.9 million to manufacturing; $2.8 million to services; and $2.5 million to government expenditures (Caribbean Business, 2026).

The early wet season drought studied in this report has the potential to drive cascading impacts for the coming months, including economic losses for farmers and low agricultural yields, increasing the likelihood for brushfires, especially if the mid-season rainfall is also low. Growing demand from urbanisation, tourism and other sectors further increases pressure on already constrained water resources (BDO, 2022).

4.2 Water management

Small island states in the Caribbean have limited freshwater reserves and often fragile water infrastructure, with many systems highly dependent on rainfall to recharge groundwater and sustain rivers (Mycoo & Roopnarine, 2024). Unregulated groundwater extraction and overextraction compounds these pressures. imited capacity to buffer periods of reduced rainfall means that drought conditions can rapidly translate into water management crises, sometimes within weeks of the onset of rainfall deficits (CARDI, 2012, Climate Risks, 2026). For example, in Jamaica, groundwater accounts for approximately 84% of the water supply, while changes in rainfall patterns and increasing demand are affecting aquifer recharge (Forde, Cashman & Mitchell, 2024). At the same time, ageing infrastructure, leakage, inaccurate metering, inadequate management practices and water theft reduce the amount of water available to users in many Caribbean islands (Nibbs, 2024, ASCE, 2019). Water losses average around 46% across the Caribbean, and can reach 75% in some areas (Janson et al., 2021).,

Water management on small islands in the Caribbean consist of a mix of longer-term practices, such as watershed rehabilitation and protection, infrastructure restoration, and rainwater harvesting, as well as emergency measures, including water conservation orders and water rationing schedules (FAO, 2019; Coley-Graham, 2021; Nelson, 2025; Méndez Tejada, 2026). Jamaica, for example, is constructing 65 kilometres of new transmission pipelines through the Western Water Resilience project to reduce leakage and increase available supply (Vinci, 2026). However, this does not fully address the underlying dependence on individual reservoirs serving large metropolitan areas (CNW, 2026). Increasing pressures highlight the need to move beyond reactive drought response towards proactive, climate-smart water management. This includes incorporating climate projections into hydrological planning and modelling, strengthening infrastructure and reducing system losses, diversifying water sources, and reassessing approaches to wastewater management and reuse (Jimenez & Bray, 2022).

4.3 Livelihoods and food security

Livelihoods across Caribbean islands are largely focused on tourism and hospitality, construction agriculture, fishing, and aquaculture, many of which are considered informal. Informal employment rates are at 54.6% in Jamaica and 48.1% in Grenada (ILO, 2023a, 2023b), with over 20% of Puerto Rico's economy categorized as informal (Bond et al., 2020). This can have significant implications for the earning capabilities of many professions that are impacted by drought, such as street vendors, seasonal farmworkers, and small-scale farmers or fishers,unlike for salaried workers (Devdiscourse). Shares of the workforce engaged in the agricultural sector range from about 1-2% (Puerto Rico) to 15-21% (Jamaica and parts of the Lesser Antilles, notably Dominica) (World Bank, 2025; 2023; Agribbean Agribusiness, n.d.). Farming remains central to food security, rural economies and is the livelihood most vulnerable to drought due to high reliance on rain and low use of irrigation systems (Buckland & Campbell, 2021, Rhiney, Eitzinger & Farrell, 2016). Using drought-tolerant seeds, investing in irrigation infrastructure and further research on drought-tolerant cultivars are potential adaptations to drought (Gould et al., 2015).

In Jamaica, productive agricultural land is concentrated among relatively few large farms. Smallholders producing domestic crops often operate on less productive land, and poverty is strongly associated with drought exposure (FAO, 2024). In Grenada, 80% of farmers producing domestic crops are smallholder producers, many operating without formal land titles (FAO, 2024). In Puerto Rico the majority of farms are individual or family-owned, and only about 16% have crop insurance, while over half have a household income under 20,000 USD (Gould et al, 2015). The crops grown by Puerto Rican farmers such as coffee are also affected by higher temperatures and drought, leading to lower quality yields (Gould et al, 2015). Therefore, farmers are at high risk of socioeconomic impacts from droughts. Droughts also impact livestock by reducing the quality and availability of fodder, and requiring farmers to depend on buying feed whose price increases during a drought (Gould et al, 2015).

Reduced water availability can also stress dairy cattle and reduce production (Gould et al, 2015).

The Caribbean has the highest cost of a healthy diet compared to the global estimate (FAO, 2025). Current estimates indicate that 20–50% of Caribbean populations experience food insecurity, disproportionately affecting lower-income groups (WFP/UN, FAO, 2025, Taller Salud, 2025). Food insecurity encompasses not only availability diminished by drought, but also access, utilisation and stability (Moraes et al., 2023). Food security vulnerabilities in the Caribbean are also gendered. Moderate to severe food insecurity is 5% higher among women than men, the largest gender gap globally (FAO, 2025). Structural inequalities can further compound these risks. For example, although women typically have formal legal equality in land rights, female-headed households remain overrepresented among poorer groups and have limited effective access to land, as documented in Jamaica (FAO, 2024).

4.4 Drought risk management

Drought risk management adopts a three-pillar approach to assess and respond to drought risk: (1) monitoring, early warning and prediction, (2) vulnerability, resilience and impact assessment, and (3) mitigation and response planning (UNDRR, 2021). In the Caribbean, regional and national disaster management and forecasting and monitoring agencies have advanced in monitoring, forecasting, and mitigation efforts following an intense drought event in 2009-2010 (Trotman et al., 2021).

4.4.1 Governance, policies and plans

Across the Caribbean, drought is managed through different levels of government. The Caribbean Institute for Meteorology and Hydrology (CIMH) coordinates the Caribbean Drought and Precipitation Monitoring Network (CDPMN), a regional operational network of national hydrological and meteorological services which provide regional drought monitoring and drought bulletins (Trotman et al., 2021). The Caribbean Disaster Emergency Management Agency (CDEMA) coordinates disaster risk reduction through its Comprehensive Disaster Management (CDM) (CDEMA, 2026). However, not all Caribbean countries are CDEMA participating states. For example, Jamaica, Grenada, St Kitts and Nevis, St Vincent and the Grenadines, St Lucia and US Virgin Islands (US territory) are CDEMA participating states, whereas Puerto Rico (US territory) and Bermuda (UK overseas territory) fall outside the formal CDEMA/CDM participating state framework.

Several CDEMA-participating states have local national drought management plans or drought-inclusive Integrated Water Resources Management (IWRM) plans that align with the CDM. For example, Jamaica's drought risk management is governed by the Water Sector Policy (2019) and overseen by a multistakeholder Drought Management Committee under the Integrated Water Resource Management Council (IWRMC) (Jamaica Information Service, 2026). Others like Grenada and St Lucia, have dedicated drought management plans

(Government of Grenada, 2019. Drought mitigation is also incorporated into broader national and sectoral planning frameworks. In St Kitts and Nevis, the Nevis Physical Planning Department adopted and implemented the Nevis Physical Planning and Development Control Regulations (2021), which require buildings intended for human habitation to have minimum water-storage capacity (FAO, 2024). Similarly, building codes in the U.S. Virgin Islands require self-sustaining water supply systems or rainwater collection in non-commercial buildings (V.I. Code tit. 29, § 308 2025).

While strides have been made, drought management planning and IWRM adoption remains uneven across the Caribbean with implementation and operational barriers and challenges across sectors (FAO, 2016, GWP-C, 2026). The responsibilities of sustainable development, disaster risk reduction and climate change adaptation policies are also given to different institutions, which remain mostly siloed with conflicting mandates and competing interests (UNDRR, 2023). Like many small island states, Caribbean states struggle with a lack of funding, low priority of risk management initiatives (Roopnarine et al., 2021) and high rates of water losses due to weak infrastructure governance (Forde, Cashman and Mitchell, 2024).

Although Puerto Rico and the US Virgin Islands are within the broader CDPMN coverage as US territories, their primary monitoring is conducted through the U.S. National Integrated Drought Information System (NIDIS), with the U.S. Drought Monitor providing the standard drought classification (NIDIS, 2026). In Puerto Rico, the Drought protocol (2015) (*Protocolo Para el Manejo de Sequía en Puerto Rico*) establishes institutional arrangements linking federal drought monitoring and response by Puerto Rico Aqueduct and Sewer Authority (AAA/PRASA) and the Department of Natural and Environmental Resources (DRNA/DNER), with emergency coordination by the Bureau for Emergency Management and Disaster Administrations (Puerto Rico Scientific Committee on Droughts, 2015). Puerto Rico's drought management is also closely tied to broader water-resource planning and allocation, reservoir management and the Puerto Rico Aqueducts and Sewer Authority system, as outlined in the Comprehensive Water Resources Plan (Instituto de Estadisticas de Puerto Rico, 2008). Historically persistent drought vulnerability has been linked to rainfall deficits and infrastructure-focused approaches to water management. However, planning, allocation and Puerto Rico's political-economic system have also contributed to increased vulnerability (García-López & Cruz-Martínez, 2015). Government programs are designed to reduce vulnerabilities and enhance capacity and resilience but many actions may not reach areas of highest exposure (Álvarez-Berríos et al., 2018). As U.S. territories, Puerto Rico and the U.S. Virgin Islands also rely on federal processes to access certain forms of agriculture. However, there can be a lag between drought impacts and initiation of response efforts (USDA, n.d).

4.4.2 Early warning early action

he Caribbean Climate Outlook Forum (CariCOF), coordinated by CIMH, provides several drought early-warning products geared towards multi-sectoral decision support (Trotman et al., 2021). The Drought Outlook provides forecasts that are updated every month using six (short-term drought) and twelve month (long-term drought) Standardised Precipitation Index (SPI) forecasts (CIMH, n.d.). The Climate Outlook newsletter and bulletin communicate threat levels, consensus climate, rainfall, temperature, and drought forecasts, alongside headline risk assessments for the region (CIMH, n.d.).

In February, long-term drought outlook forecasted emergencies for Grenada and St Lucia with drought warnings issued for other islands including St Kitts, Martinique and Dominica up to the end of May (Figure 4.4.2.1).

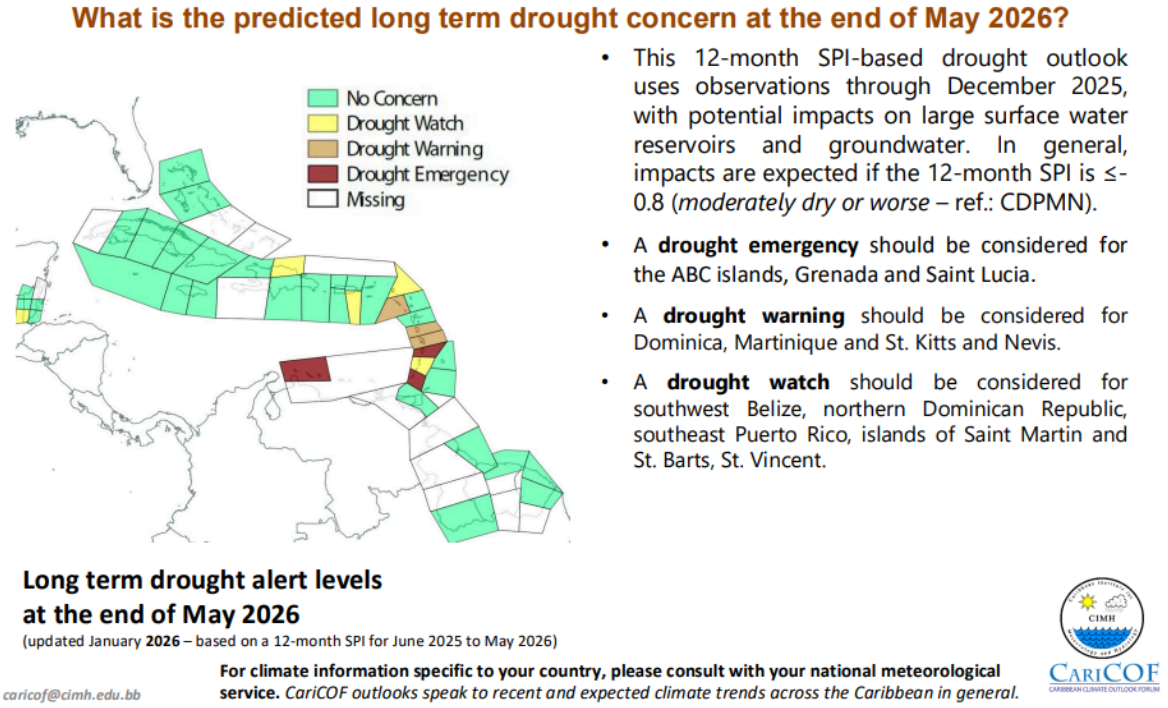


Figure 4.4.2.1: *Feb 2026 CARICOF outlook: Predicted long-term drought concern by end of May Source: CIMH, 2026 Feb*

By April 2026, drought emergency forecasts persisted for Grenada, St Lucia and Saint Kitts, while drought warnings were in place for Aruba, Bonaire and Curacao (ABC) islands, southern Belize, Dominica and Martinique (Figure 4.4.2.2) (CIMH, April 2026). St Lucia, Grenada and St Vincent all reported lower than normal river levels at the beginning of 2026, following below-average surface water and groundwater resources during the 2025 wet season (ISVG, 2026).

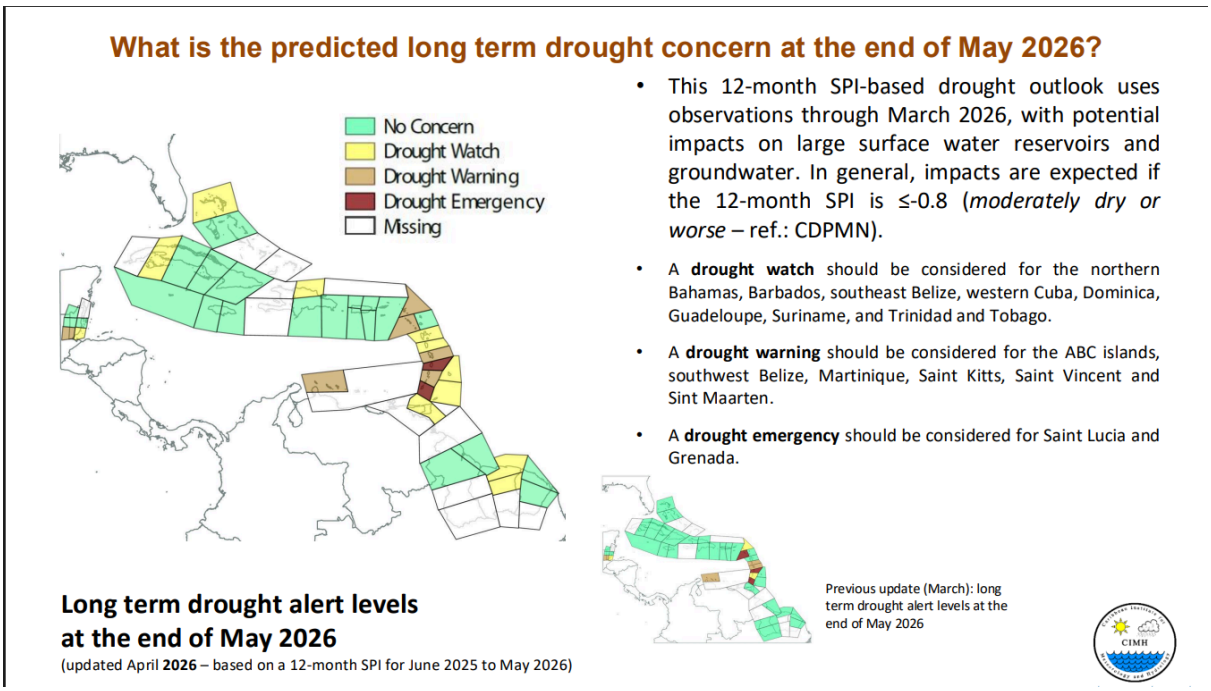


Figure 4.4.2.2: *April 2026 CARICOF outlook predicted long-term drought concern by the end of July 2026 Source: CIMH, 2026 April*

At the country level, drought warnings are communicated by local meteorological, water resources and agricultural agencies and disseminated through various online and media avenues (Buckland & Campbell, 2021). In January, agencies urged residents, businesses and farmers to adopt water conservation as part of seasonal preparedness measures (ISVG, 2026, MoALSU, Jan 2026). In St Lucia, residents were also urged to invest in rainwater harvesting to increase water storage (Saint Lucia Daily Post, Jan 2026). However, there can often be a disconnect between receiving warnings and taking action at community or household levels. For example, in Jamaica, 98% of farmers reported receiving forecasts and warnings, but only a third changed their farming practices accordingly (Buckland & Campbell, 2021).

For Puerto Rico and the US Virgin Islands, drought monitoring and forecasting are integrated into the U.S. NOAA/National Weather Service (NWS) system, with NOAA's National Integrated Drought Information System (NIDIS) coordinating and providing drought information and early-warning services through Drought.gov. NOAA's Climate Prediction Centre (CPC) Seasonal drought outlooks valid for April 30th to July 31st 2026 did not predict drought conditions for Puerto Rico and US Virgin Islands (NOAA, April 2026). Monthly drought outlooks also indicated no drought up until the June 30th monthly outlook, which predicted droughts in southern parts of Puerto Rico in July (NOAA, June 2026).

4.4.3 Emergency response and coping strategies

Government agencies have implemented several measures in response to these drought impacts, including water distribution. In St Lucia, the Water Supply Agency (WASCO) intensified the trucking of potable water to essential services and the most impacted communities and continued valving operations to help ensure more equitable distribution across affected districts (St Lucia Times, 2026, Caribbean Risks, 2026). Communities at the higher elevations at the farthest end of the network are also the most affected (St Lucia Times, 2026). The Saint Vincent and the Grenadines (SVG) Red Cross and Water Mission, in partnership with local NGOs assisted with water distributions to the island of Bequia and Union Island in the Grenadines where there are no rivers and heavy reliance on rainwater harvesting (IFRC/SVGRC, 2026).

In Puerto Rico, declining levels in the Carraízo reservoir, the main source of water for the metropolitan area, have resulted in water rationing affecting approximately 500,000 people, while other reservoirs are being closely monitored (Maturana, 2026). Authorities implemented 48 hour rotating water rationing for more than 180,000 customers, deployed water trucks and National Guard support, and prioritized water access to hospitals and elderly residents, while FEMA supplied emergency water trailers (Florido, 2026).

As of August 17th, Jamaica's National Water Commission (NWC) Water Prohibition Order, prohibits the use of water for non-essential or unusual purposes (Jamaica Information Service, 2026).However, there can be challenges during water rationing for islands dependent on tourism, where water can be diverted to hotels and other sites potentially worsening shortages for local communities (Nibbs, 2024).

Jamaica's Government has also allocated emergency funding (about $60 million JMD/ 300K USD) for water trucking for farmers, drip irrigation, storage tank, catchment ponds to increase resilience (MoAJM, 2026). Timely delivery of support can help farmers implement measures before water shortages translate into significant agricultural losses. During past droughts, farmers have implemented coping strategies such as mulching to reduce moisture loss, borrowing money to buy water, or sacrificing a portion of crops under cultivation (Campbell et al., 2011). During the 2014 drought in Jamaica farmers who had storage capacity shared water with those who didn't, highlighting the importance of social networks and capital and responding to the drought (Moulton et al., 2015).

Household coping strategies can vary greatly by socioeconomic status. Higher income households use cisterns, private water trucking, and diverse income sources to manage shocks. In contrast, poorer and older residents often depend on manual water hauling and informal support, which can place them at higher health and logistical risks (Florido, 2026). Social capital, including neighbourhood-level sharing of water and informal mutual aid, plays a meaningful buffering role where formal systems are strained

4.4.4 Insurance

Expansion of drought insurance in the Caribbean is an emerging risk management strategy. In 2020, Puerto Rico's insurance commissioner established "Regla 103", a regulation to enable parametric microinsurance for low-income families affected by disasters (OCS, 2020). In 2023, they published "Regla 105" that strengthened the previous framework, expanding the insurance coverage and including commercial parametric insurance (OCS, 2023).Similarly, in 2021, Jamaica's Ministry of Agriculture, Fisheries and Mining launched GK Weather Protect, a crop insurance policy that provides coverage to farmers and fishers for losses from heavy rain, hurricane winds and droughts (MOA, 2021). In 2026, they expanded the coverage, transitioning from the parametric scheme to year-round coverage against hurricane winds, excess rainfall, and drought, eliminating the need for farmers to reapply each season (JIS, 2026).

In 2025, St. Lucia's Ministry of Agriculture announced an agreement with GK Insurance Limited to set up a landmark insurance scheme for registered banana and plantain farmers, the government will contribute a one-time payment of $1 million, which provides coverage for wind damage caused by Tropical Storms and Hurricanes (Government of St. Lucia, 2025). To date, there is no specific insurance scheme for droughts. This is also the case in St. Vincent and the Grenadines and Grenade, where risks are managed through the CCRIF SPC parametric insurance, but do not include droughts. Even at a regional level, the Caribbean Catastrophe Risk Insurance Facility (now CCRIF SPC) does not cover drought impacts as of now (CCRIF SPC, n.d.).

4.5 Adaptation measures

Appropriate adaptation measures for drought vary depending on the specific island context including factors like governance, availability of ground water, geology, and financial viability.

Several countries, including Barbados, Guyana, Grenada, Saint Lucia and Jamaica, have developed or are implementing national water information systems to support planning and demand management, often with external donor financing given persistent fiscal constraints across the region (IADB, 2013). According to one study of over 300 farmers in Jamaica, those who had access to climate information services reported lower crop losses and financial strain and were more likely to reinvest after drought events (Buckland and Campbell, 2022).

Water scarce islands such as Barbados, Antigua and Barbuda, and Saint Kitts and Nevis rely heavily on diversified supply sources, including rainwater harvesting (near-total dependence for parts of the Grenadines) and desalination (IADB, 2013). Puerto Rico's 2026 rationing crisis highlights substantial system losses and untapped opportunities, with approximately 60% of treated water estimated as being lost through leakage before delivery (Funes, 2026). Expanded household-scale rainwater harvesting and harnessing stormwater could potentially

capture billions of gallons annually and ease pressure on a centralized system vulnerable to disruption (Yang et al., 2025).

It is also important to integrate traditional knowledge into drought adaptation practices. For example, communities in the Lesser Antilles have relied on drought adaptation practices sustained over centuries including relocation to more resilient settlement sites during dry periods, buried clay pot water catchments, and observation of environmental cues, such as lunar phases and plant flowering, to anticipate dry spells (Hofman et al. 2021). Kalinago and Garifuna communities in Dominica and Saint Vincent continue to draw on this traditional knowledge for water security alongside contemporary institutional systems, though the authors note such knowledge remains underutilised in formal climate adaptation planning and ecosystem-based adaptation (Hofman et al. 2021; Mercer et al., 2012). Further, drought information is more likely to be adopted by farmers if created and shared through open, transparent and participatory processes (Gould et al., 2015).

The IPCC highlights drip irrigation technologies, growing drought resistant crops, watershed management and conservation as potential adaptation solutions to drought in the Caribbean (Mycoo et al., 2021). However, for many small islands, adaptation remains constrained by a lack of financing, institutional capacity, and technology to support effective implementation (Mycoo et al., 2021). Literature on adaptation to droughts for specific Caribbean islands is limited and largely focused on case studies. More research is required to fully assess viable adaptation options, better understand the feasibility of these options in practice and characterise the nuances for different islands and communities.

5 Conclusions

Overall, we find a decreasing trend in early wet season precipitation over Jamaica and Puerto Rico. We do not see an increase in potential evapotranspiration, or a stronger trend in effective precipitation over precipitation only – as might be expected with the trend towards higher temperatures. This means that the increasing severity of both meteorological and ecological droughts can be explained almost entirely by the decrease in precipitation in dryer May-July periods. Trends were mixed and highly uncertain over the Lesser Antilles – reinforcing the already clear need for expanded monitoring schemes over small islands and the improved representation of them in gridded weather products and climate models.

The increasing likelihood of early wet season droughts like this year's impacts water security and agricultural production in the region, and also preconditions the intensification of these impacts if drought conditions persist further into the wet season – on which climate modes such as ENSO may exert a greater influence on drought (Clarke et al., 2026). Further intensification of the drought can create cascading impacts, reducing the viability of tourism activities, a key source of income for many islands, along with a variety of social and health impacts that could occur with continued water rationing. In the long term, this

disproportionately impacts the most vulnerable people with the least means to adapt, and requires further research on island-specific adaptation solutions that can ensure water security in this region.

Data availability

All time series used in the attribution analysis are available via the Climate Explorer.

Acknowledgements

The findings and conclusions in this publication are the author's and should not be taken as official determinations or policies of the USDA or the U.S. government.

This work used JASMIN, the UK's collaborative data analysis environment (https://www.jasmin.ac.uk).

This work used resources of the Deutsches Klimarechenzentrum (DKRZ), granted by its Scientific Steering Committee (WLA) under project ID bk1088 and datasets provided by ESGF and Copernicus via the DKRZ data pool.

This work used Imperial College Research Computing Service, DOI: 10.14469/hpc/2232.

This work used the KNMI Climate explorer web tool (https://climexp.knmi.nl/start.cgi).

References

All references are given as hyperlinks in the text.

Appendices

A0 Drought Observations

PR station-based anomalies by climate region:

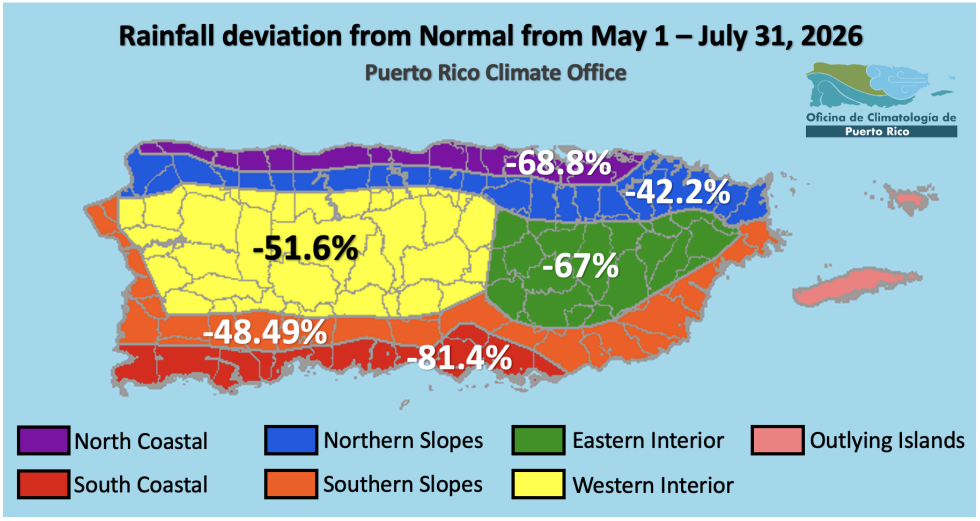


Figure A0.1*: station derived precipitation deficits over Puerto Rico for May to July.*

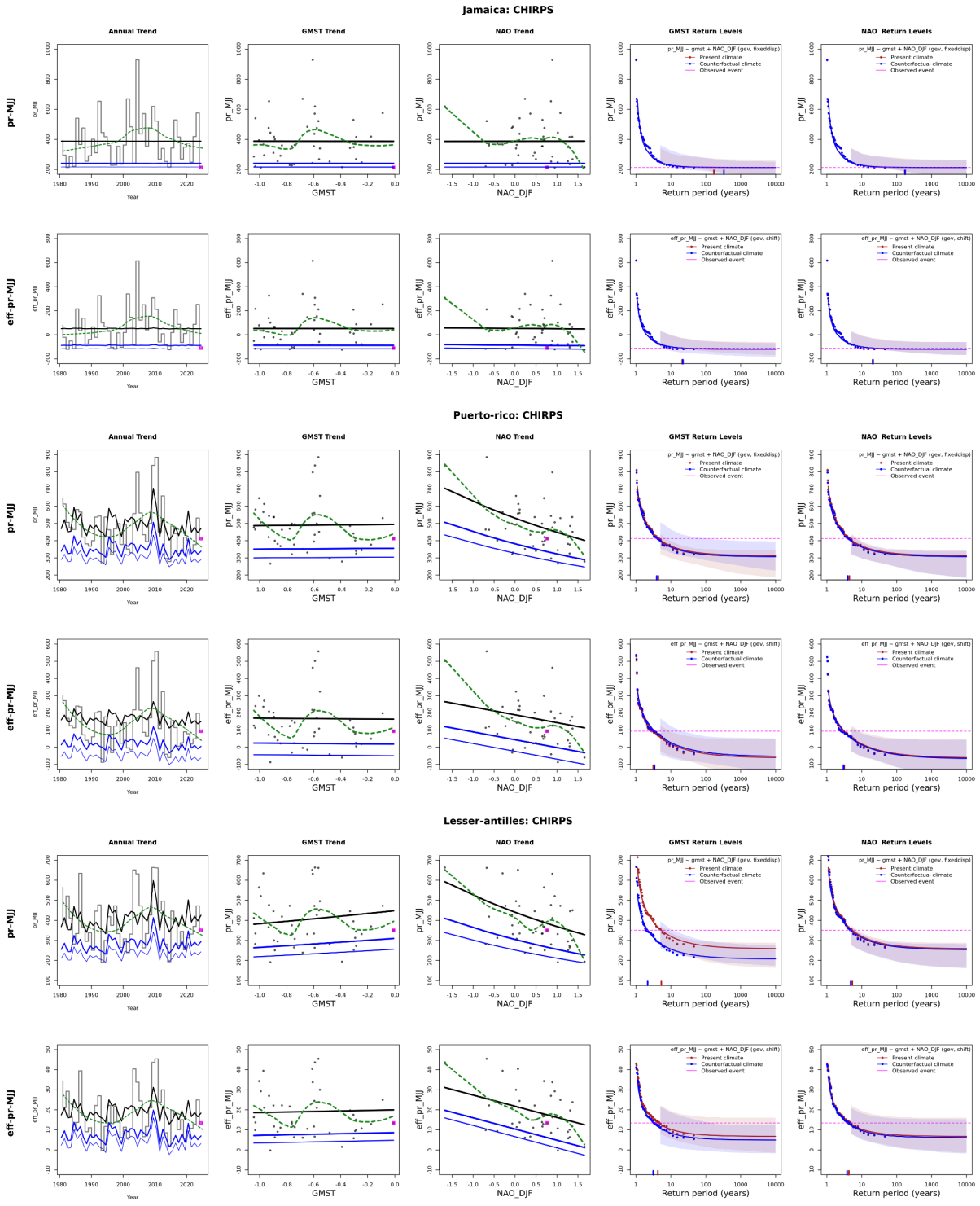


Figure A0.2*: CHIRPS/CHIRTS fits corresponding to those of MSWEP/MSWX in figures 2.1.2.1, 2.1.3.1, 2.1.4.1.*

A1 Data and methods

A1.1 Observational data

We first use observational and reanalysis data to estimate the return period of a similar event in the present day and to assess the historical trends with increasing GMST. The datasets used are as follows:

MSWX - The Multi-Source Weather dataset (Beck et al., 2022), which combines various observational and reanalysis-based data (including ERA5) for reliable bias-corrected weather variable estimates, at 3-hourly intervals from 1979 to near real-time, and at 0.1° spatial resolution globally. We use minimum and maximum temperatures data from this product.

MSWEP - The Multi-Source Weighted-Ensemble Precipitation v2.8 dataset (updated from Beck et al., 2019) is fully global, available at 3-hourly intervals and at 0.1° spatial resolution, available from 1979 to ~3 hours from real-time. This product combines gauge-, satellite-, and reanalysis-based data, including ERA5.

CHIRPS/CHIRTS - The rainfall product developed by the UC Santa Barbara Climate Hazards Group called "Climate Hazards Group InfraRed Precipitation/Temperature with Station data" (CHIRPS; Funk et al., 2015; Funk et al., 2020). Daily data are available at 0.05° resolution, from 1981-30 June 2026. The product incorporates satellite imagery with in-situ station data.

Covariates

As a measure of anthropogenic climate change we use the (low-pass filtered) global mean surface temperature (GMST), where GMST is taken from the National Aeronautics and Space Administration (NASA) Goddard Institute for Space Science (GISS) surface temperature analysis (GISTEMP, Hansen et al., 2010 and Lenssen et al. 2019). To remove the effect of the El Niño - Southern Oscillation on global mean temperatures, we use a four-year running mean of the GMST, centred on the third year.

The North Atlantic Oscillation is calculated as the difference in the Mean Sea Level Pressure (MSLP) between two boxes located around Iceland (25W-16W, 63N-70N) and the Azores (28W-20W, 36N-40N) consistent with Dunstone et al. (2016). The normalised NAO series is averaged through the extended winter season October to March.

A1.2 Model and experiment descriptions

We use 28 ensembles of climate models from climate modelling experiments using very different framings (Philip et al., 2020): Sea Surface Temperature (SST) driven global circulation high resolution models, coupled global circulation models and regional climate models.

CORDEX

Coordinated Regional Climate Downscaling Experiment CORDEX-CORE for Central America (models with at 0.44° resolution (CAM-44) and models at 0.22° resolution (CAM-22)) multi-model ensemble (Giorgi et al 2012; Giorgi et al., 2021), comprising 14 simulations resulting from pairings of Global Climate Models (GCMs) and Regional Climate Models (RCMs)). These simulations are composed of historical simulations up to 2005, and extended to the year 2100 using the RCP8.5 scenario.

2. HighResMIP SST-forced model ensemble (Haarsma et al. 2016), the simulations for which span from 1950 to 2050. The SST and sea ice forcings for the period 1950-2014 are obtained from the 0.25° x 0.25° Hadley Centre Global Sea Ice and Sea Surface Temperature dataset that have undergone area-weighted regridding to match the climate model resolution. For the 'future' time period (2015-2050), SST/sea-ice data are derived from RCP8.5 (CMIP5) data, and combined with greenhouse gas forcings from SSP5-8.5 (CMIP6) simulations (see Section 3.3 of Haarsma et al. 2016 for further details).

A1.3 Statistical methods

Methods for observational and model analysis and for model evaluation and synthesis are used according to the World Weather Attribution Protocol, described in Philip et al., (2020), with supporting details found in van Oldenborgh et al., (2021), Ciavarella et al., (2021), Otto et al., (2024) and here. The key steps, presented in sections 3-6, are: (3) trend estimation from observations; (4) model validation; (5) multi-model attribution; and (6) synthesis of the attribution statement.

In this report we analyse time series of May-July precipitation and effective precipitation (with potential evapotranspiration calculated according to the Hargreaves method).

A nonstationary GEV distribution is used to model both variables. For precipitation, the distribution is assumed to scale exponentially with the covariates, with the dispersion (the ratio between the standard deviation and the mean) remaining constant over time; while for effective precipitation, the distribution is assumed to shift linearly with the covariates, while the variance remains constant. The parameters of the statistical model are estimated using maximum likelihood.

For each time series we calculate the return period and intensity of the event under study for the 2026 GMST and for 1.4°C cooler GMST: this allows us to compare the climate of now and of the preindustrial past without human-caused warming (based on Forster et al., 2026), by calculating the probability ratio (PR; the factor-change in the event's probability) and change in intensity of the event.

In order to examine the effect of the DJF NAO phase on (effective) precipitation alongside that of increasing GMST, we extend the nonstationary model to accommodate an additional

covariate. All results quoted are from a statistical model including both covariates, with the DJF value assuming the configuration in this year.

The variable of interest, X, is assumed to follow a GEV distribution in which the location and scale parameters vary with both GMST and ENSO:

$$X \sim GEV(\mu, \sigma, \xi \mid \mu_0, \sigma_0, \alpha, \beta, T, I),$$

where X denotes the variable of interest, rainy-season precipitation; T is the smoothed GMST; I is the detrended Niño3.4 index; μ_0, σ_0 and ξ are the location, scale and shape parameters of the nonstationary distribution; and α, β are the trends due to GMST and ENSO, respectively. As a result, the location and scale of the distribution have a different value in each year, determined by both the GMST and Niño3.4 states. Maximum likelihood estimation is used to estimate the model parameters, with

$$\mu = \mu_0 exp\left(\frac{\alpha T + \beta I}{\mu_o}\right) \qquad \text{and} \qquad \sigma = \sigma_0 exp\left(\frac{\alpha T + \beta I}{\mu_o}\right).$$

This formulation reflects the Clausius Clapeyron relation, which implies that precipitation scales exponentially with temperature (Trenberth et.al., 2003, O'Gorman and Schneider 2009), and so that precipitation will scale exponentially with the strength of the detrended Niño3.4 index. Under this model, the effects of GMST and the detrended Niño3.4 index are assumed to be independent of one another, so that the change in intensity due to GMST is unaffected by the change in intensity due to the ENSO phase. We note that this may not be the case in the real world, as the intensity and frequency of El Niño events may have been influenced by climate change (Cai et al., 2021); however, by using a detrended Niño3.4 index (see Section 2.1) we aim to minimise the correlation between the two factors, and so do not expect the qualitative findings of this study to be affected by this simplifying assumption.

Extra care must be taken when reporting and interpreting return periods that depend on more than one covariate. Typically, WWA reports estimated return periods for the event of interest under current climatic conditions: that is, with the GMST fixed at the 2026 level. In this study, there are two covariates to consider: the GMST and IOD. By fixing both the IOD and the GMST at their 2024 levels, we can estimate the return period of the 2024 event in the current climate and in the current IOD state. Mathematically, this return period is written as

$$1 / P(X > x_{2024} \mid T = t_{2024}, D = d_{2024}),$$

where x_{2024} is the 2024 value of observed precipitation; t_{2024} denotes the 2024 GMST; and d_{2024} denotes the 2024 IOD. Altogether, the expression in brackets gives the probability that

X will exceed x_{2024}, given that $T = t_{2024}$ and $D = d_{2024}$; inverting this probability gives us an expected return period, in years.

However, this return period only tells us the probability of experiencing a similar event under current IOD conditions and current warming levels. In order to understand how frequently such an event is actually likely to occur, we must account for the fact that the IOD is not often in the strongly positive phase observed in 2024. To do this, we evaluate the return period over all states of the IOD that have been recorded since 1980 (the period covered by the available gridded data products). This is done by first averaging the probability of exceeding x_{2024} over all recorded values of d_{2024} during this period, then inverting to obtain the return period:

$$1 / \sum_{y=1980}^{2024} P(X > x_{2024} \mid T = t_{2024}, D = d_y).$$

A1.3.3 Defining the NAO state in climate models

The multi-model attribution step of the WWA protocol involves estimating, for each climate model, the effective return level of a 1-in-*n*-year event under the current climate state, and estimating the expected change in likelihood and intensity of such an event after a specified change in the covariates. Because the smoothed GMST is generally monotonically increasing, the standard WWA approach is simply to take the model's 2026 GMST as a covariate and to estimate the expected magnitude of an *n*-year event. However, the factual climate in this study is defined by the 2026 GMST and by the value of the detrended DJF NAO index.

A2 Model evaluation tables

Table A2.1 Evaluation results of the climate models considered for attribution analysis of Jamaica pr-MJJ. For each model, the best estimates of the Dispersion and Shape parameters are shown, along with a 95% confidence intervals. Furthermore evaluation of the seasonal cycle and spatial pattern are shown.

Model / Observations	Seasonal cycle	Spatial pattern	Dispersion	Shape parameter
CHIRPS			0.490 (0.251 ... 0.457)	-1.1 (-0.98 ... -0.40)
MSWEP			0.356 (0.240 ... 0.483)	-0.43 (-0.88 ... -0.23)
CORDEX				
CORDEX_CanESM2-CRCM5_r1	reasonable	good	0.164 (0.125 ... 0.193)	-0.31 (-0.67 ... -0.17)
CORDEX_CanESM2-RCA4_r1	reasonable	good	0.183 (0.124 ... 0.233)	-0.23 (-0.48 ... 0.092)
CORDEX_CNRM-CM5-RCA4_r1	good	good	0.261 (0.194 ... 0.312)	-0.46 (-0.77 ... -0.28)

CORDEX_EC-EARTH-RCA4_r12	good	reasonable	0.156 (0.120 ... 0.194)	-0.41 (-0.87 ... -0.15)
CORDEX_GFDL-ESM2M-RCA4_r1	good	reasonable	0.211 (0.161 ... 0.269)	-0.35 (-0.64 ... -0.19)
CORDEX_GFDL-ESM2M-RegCM4-7_r1	good	good	0.226 (0.162 ... 0.305)	-0.42 (-0.78 ... -0.15)
CORDEX_HadGEM2-ES-RCA4_r1	good	good	0.200 (0.129 ... 0.287)	-0.14 (-0.55 ... 0.31)
CORDEX_HadGEM2-ES-RegCM4-7_r1	good	good	0.249 (0.172 ... 0.319)	-0.51 (-0.95 ... -0.23)
CORDEX_IPSL-CM5A-MR-RCA4_r1	bad	reasonable	0.315 (0.223 … 0.379)	-0.412 (-0.85 … -0.14)
CORDEX_MIROC5-RCA4_r1	reasonable	reasonable	0.290 (0.152 ... 0.317)	-0.96 (-0.97 ... -0.24)
CORDEX_MPI-ESM-LR-RCA4_r1	good	good	0.263 (0.183 ... 0.332)	-0.45 (-0.77 ... -0.086)
CORDEX_MPI-ESM-LR-REMO2015_r1	good	good	0.323 (0.238 ... 0.399)	-0.42 (-0.89 ... -0.17)
CORDEX_MPI-ESM-MR-RegCM4-7_r1	good	good	0.181 (0.124 ... 0.203)	-0.33 (-0.83 ... -0.11)
CORDEX_NorESM1-M-RCA4_r1	good	good	0.207 (0.146 ... 0.253)	-0.61 (-0.95 ... -0.31)
CORDEX_NorESM1-M-REMO2015_r1	bad	reasonable	0.493 (0.318 … 0.626)	-0.628 (-0.90 … -0.25)
HighResMIP				
HighResMIP_CNRM-CM6-1_r1	reasonable	reasonable	0.471 (0.314 ... 0.589)	-0.60 (-0.91 ... -0.27)
HighResMIP_CNRM-CM6-1-HR_r1	reasonable	reasonable	0.298 (0.212 ... 0.387)	-0.58 (-0.92 ... -0.32)
HighResMIP_EC-Earth3P_r2	good	good	0.381 (0.284 ... 0.466)	-0.61 (-0.85 ... -0.37)
HighResMIP_EC-Earth3P_r3	good	good	0.285 (0.212 ... 0.370)	-0.41 (-0.74 ... -0.19)
HighResMIP_EC-Earth3P-HR_r2	good	good	0.268 (0.200 ... 0.334)	-0.48 (-0.77 ... -0.29)
HighResMIP_EC-Earth3P-HR_r3	good	good	0.218 (0.152 ... 0.270)	-0.39 (-0.73 ... -0.13)
HighResMIP_HadGEM3-GC31-HM_r1	reasonable	good	0.194 (0.140 ... 0.234)	-0.26 (-0.66 ... -0.051)
HighResMIP_HadGEM3-GC31-HM_r1	reasonable	good	0.229 (0.151 ... 0.280)	-0.39 (-0.60 ... -0.070)
HighResMIP_HadGEM3-GC31-MM_r1	reasonable	good	0.353 (0.233 ... 0.439)	-0.58 (-0.88 ... -0.26)
HighResMIP_MPI-ESM1-2-XR_r1	reasonable	good	0.268 (0.162 ... 0.325)	-0.45 (-0.83 ... -0.088)

Table A2.2: Evaluation results of the climate models considered for attribution analysis of Lesser Antilles pr-MJJ. For each model, the best estimates of the Dispersion and Shape parameters are shown, along with a 95% confidence intervals. Furthermore evaluation of the seasonal cycle and spatial pattern are shown.

Model / Observations	**Seasonal cycle**	**Spatial pattern**	**Dispersion**	**Shape parameter**
CHIRPS			0.290 (0.224 ... 0.374)	-0.60 (-0.94 ... -0.38)
MSWEP			0.300 (0.230 ... 0.371)	-0.57 (-0.94 ... -0.36)
CORDEX				
CORDEX_CanESM2-CRCM5_r1	reasonable	good	0.141 (0.0953 ... 0.171)	-0.56 (-0.91 ... -0.28)
CORDEX_CanESM2-RCA4_r1	reasonable	good	0.285 (0.204 ... 0.350)	-0.39 (-0.68 ... -0.13)
CORDEX_CNRM-CM5-CRCM5_r1	good	good	0.235 (0.105 ... 0.287)	-0.60 (-0.87 ... -0.017)
CORDEX_EC-EARTH-RCA4_r12	good	reasonable	0.276 (0.196 ... 0.336)	-0.39 (-0.61 ... -0.17)
CORDEX_GFDL-ESM2M-RCA4_r1	good	reasonable	0.234 (0.149 ... 0.290)	-0.47 (-0.77 ... -0.064)
CORDEX_GFDL-ESM2M-RegCM4-7_r1	good	good	0.460 (0.312 ... 0.560)	-0.67 (-0.92 ... -0.34)
CORDEX_MIROC5-RCA4_r1	reasonable	reasonable	0.384 (0.288 ... 0.475)	-0.59 (-0.93 ... -0.38)
CORDEX_MPI-ESM-LR-RCA4_r1	good	good	0.331 (0.242 ... 0.402)	-0.49 (-0.80 ... -0.28)
CORDEX_MPI-ESM-LR-REMO2015_r1	good	good	0.255 (0.152 ... 0.324)	-0.25 (-0.51 ... 0.23)
CORDEX_MPI-ESM-MR-RegCM4-3_r1	good	reasonable	0.431 (0.286 ... 0.541)	-0.53 (-0.94 ... -0.23)
CORDEX_MPI-ESM-MR-RegCM4-7_r1	good	good	0.468 (0.259 ... 0.516)	-0.83 (-0.97 ... -0.28)
CORDEX_NorESM1-M-RCA4_r1	good	good	0.365 (0.214 ... 0.483)	-0.57 (-0.93 ... -0.15)
CORDEX_NorESM1-M-REMO2015_r1	good	good	0.357 (0.239 ... 0.444)	-0.43 (-0.66 ... -0.13)
HighResMIP				
HighResMIP_CNRM-CM6-1_r1	reasonable	reasonable	0.301 (0.215 ... 0.380)	-0.55 (-0.87 ... -0.26)
HighResMIP_CNRM-CM6-1-HR_r1	reasonable	reasonable	0.225 (0.155 ... 0.264)	-0.24 (-0.50 ... 0.024)
HighResMIP_EC-Earth3P_r2	good	good	0.441 (0.319 ... 0.540)	-0.72 (-0.97 ... -0.48)
HighResMIP_EC-Earth3P_r3	good	good	0.501 (0.378 ... 0.553)	-0.87 (-0.98 ... -0.61)
HighResMIP_EC-Earth3P-HR_r2	good	good	0.405 (0.298 ... 0.501)	-0.62 (-0.93 ... -0.41)

HighResMIP_HadGEM3-GC31-HM_r1i2	reasonable	good	0.416 (0.304 ... 0.526)	-0.61 (-0.95 ... -0.39)
HighResMIP_HadGEM3-GC31-HM_r1i3	reasonable	good	0.385 (0.282 ... 0.480)	-0.57 (-0.84 ... -0.33)
HighResMIP_HadGEM3-GC31-LM_r1i1	reasonable	reasonable	0.478 (0.362 ... 0.553)	-0.73 (-0.96 ... -0.52)
HighResMIP_HadGEM3-GC31-MM_r1	reasonable	good	0.407 (0.274 ... 0.507)	-0.55 (-0.90 ... -0.30)
HighResMIP_MPI-ESM1-2-HR_r1	good	good	0.420 (0.322 ... 0.520)	-0.48 (-0.82 ... -0.30)
HighResMIP_MPI-ESM1-2-XR_r1	reasonable	good	0.397 (0.274 ... 0.500)	-0.44 (-0.74 ... -0.20)

Table A2.3: Evaluation results of the climate models considered for attribution analysis of Puerto Rico pr-MJJ. For each model, the best estimates of the Dispersion and Shape parameters are shown, along with a 95% confidence intervals. Furthermore evaluation of the seasonal cycle and spatial pattern are shown.

Model / Observations	**Seasonal cycle**	**Spatial pattern**	**Dispersion**	**Shape parameter**
CHIRPS			0.268 (0.172 ... 0.327)	-0.63 (-0.91 ... -0.25)
MSWEP			0.255 (0.177 ... 0.324)	-0.37 (-0.70 ... -0.14)
CORDEX				
CORDEX_CanESM2-CRCM5_r1	reasonable	good	0.211 (0.118 ... 0.274)	-0.65 (-0.97 ... -0.28)
CORDEX_CanESM2-RCA4_r1	reasonable	good	0.264 (0.174 ... 0.319)	-0.47 (-0.81 ... -0.20)
CORDEX_CNRM-CM5-CRCM5_r1	good	good	0.356 (0.223 ... 0.429)	-0.65 (-0.88 ... -0.35)
CORDEX_CNRM-CM5-RCA4_r1	good	good	0.300 (0.236 ... 0.364)	-0.43 (-0.85 ... -0.29)
CORDEX_EC-EARTH-RCA4_r12	good	reasonable	0.248 (0.176 ... 0.311)	-0.48 (-0.76 ... -0.19)
CORDEX_GFDL-ESM2M-RCA4_r1	good	reasonable	0.303 (0.224 ... 0.377)	-0.51 (-0.89 ... -0.33)
CORDEX_GFDL-ESM2M-RegCM4-7_r1	good	good	0.472 (0.340 ... 0.608)	-0.60 (-0.90 ... -0.35)
CORDEX_HadGEM2-ES-RCA4_r1	good	good	0.328 (0.232 ... 0.405)	-0.63 (-0.93 ... -0.36)
CORDEX_HadGEM2-ES-RegCM4-3_r1	bad	reasonable	0.516 (0.348 ... 0.640)	-0.65 (-0.95 ... -0.37)
CORDEX_HadGEM2-ES-RegCM4-7_r1	good	good	0.442 (0.313 ... 0.574)	-0.54 (-0.83 ... -0.31)
CORDEX_MIROC5-RCA4_r1	reasonable	reasonable	0.379 (0.253 ... 0.464)	-0.56 (-0.93 ... -0.33)

CORDEX_MPI-ESM-LR-RCA4_r1	good	good	0.339 (0.267 ... 0.417)	-0.47 (-0.88 ... -0.29)
CORDEX_MPI-ESM-LR-REMO2015_r1	good	good	0.416 (0.284 ... 0.540)	-0.60 (-0.91 ... -0.23)
CORDEX_MPI-ESM-MR-RegCM4-7_r1	good	good	0.302 (0.206 ... 0.374)	-0.50 (-0.94 ... -0.21)
CORDEX_NorESM1-M-RCA4_r1	good	good	0.253 (0.167 ... 0.327)	-0.43 (-0.84 ... -0.19)
HighResMIP				
HighResMIP_CNRM-CM6-1_r1	reasonable	reasonable	0.387 (0.263 ... 0.444)	-0.80 (-0.97 ... -0.43)
HighResMIP_CNRM-CM6-1-HR_r1	reasonable	reasonable	0.277 (0.170 ... 0.346)	-0.36 (-0.75 ... 0.057)
HighResMIP_EC-Earth3P_r2	good	good	0.451 (0.330 ... 0.534)	-0.65 (-0.93 ... -0.39)
HighResMIP_EC-Earth3P_r3	good	good	0.455 (0.367 ... 0.540)	-0.61 (-0.96 ... -0.45)
HighResMIP_EC-Earth3P-HR_r2	good	good	0.313 (0.240 ... 0.382)	-0.47 (-0.75 ... -0.28)
HighResMIP_EC-Earth3P-HR_r3	good	good	0.298 (0.214 ... 0.388)	-0.44 (-0.85 ... -0.15)
HighResMIP_HadGEM3-GC31-HM_r1i2	reasonable	good	0.334 (0.261 ... 0.396)	-0.70 (-0.97 ... -0.43)
HighResMIP_HadGEM3-GC31-HM_r1i3	reasonable	good	0.335 (0.211 ... 0.390)	-0.79 (-0.97 ... -0.34)
HighResMIP_HadGEM3-GC31-MM_r1	reasonable	good	0.266 (0.178 ... 0.341)	-0.32 (-0.63 ... 0.047)
HighResMIP_MPI-ESM1-2-XR_r1	reasonable	good	0.276 (0.206 ... 0.340)	-0.27 (-0.52 ... -0.087)

Table A2.4 Evaluation results of the climate models considered for attribution analysis of eff-pr-MJJ for each region. For each model with available data and a successful fit, the best estimates of the Sigma and Shape parameters are shown, along with a 95% confidence intervals. Furthermore evaluation of the seasonal cycle and spatial pattern are shown.

	Jamaica		**Lesser Antilles**		**Puerto Rico**	
Model / Observations	**Sigma**	**Shape parameter**	**Sigma**	**Shape parameter**	**Sigma**	**Shape parameter**
CHIRPS	167 (106 ... 204)	-0.97 (-0.98 ... -0.37)	11.3 (8.24 ... 13.6)	-0.69 (-0.97 ... -0.33)	127 (83.3 ... 170)	-0.50 (-0.94 ... -0.17)
MSWEP	181 (117 ... 226)	-0.63 (-0.94 ... -0.29)	185 (77.1 ... 126)	-1.0 (-0.97 ... -0.26)	145 (81.0 ... 157)	-0.57 (-0.82 ... -0.16)
CORDEX						
CORDEX_CanES	131 (92.1 ...	-0.27 (-0.71	105 (77.2 ...	-0.40 (-0.70 ...	136 (88.0 ...	-0.50 (-0.87 ...

M2-RCA4_r1	168)	... 0.027)	123)	-0.11)	169)	-0.25)
CORDEX_CNRM-CM5-RCA4_r1	150 (110 ... 183)	-0.44 (-0.84 ... -0.26)	106 (77.7 ... 127)	-0.54 (-0.89 ... -0.27)	169 (133 ... 206)	-0.37 (-0.87 ... -0.24)
CORDEX_EC-EARTH-RCA4_r12	123 (92.8 ... 150)	-0.47 (-0.96 ... -0.20)	121 (88.5 ... 148)	-0.39 (-0.83 ... -0.20)	169 (120 ... 205)	-0.47 (-0.76 ... -0.20)
CORDEX_GFDL-ESM2M-CRCM5_r1	112 (76.2 ... 137)	-0.60 (-0.95 ... -0.29)	57.9 (36.8 ... 71.0)	-0.53 (-0.92 ... -0.11)		
CORDEX_GFDL-ESM2M-RegCM4-7_r1	134 (95.0 ... 167)	-0.42 (-0.79 ... -0.10)			83.1 (60.5 ... 102)	-0.67 (-0.96 ... -0.40)
CORDEX_HadGEM2-ES-RCA4_r1	123 (80.9 ... 171)	-0.14 (-0.72 ... 0.35)			108 (71.5 ... 134)	-0.72 (-0.97 ... -0.47)
CORDEX_HadGEM2-ES-RegCM4-3_r1					95.2 (59.9 ... 118)	-0.74 (-0.97 ... -0.39)
CORDEX_IPSL-CM5A-MR-RCA4_r1	94.0 (67.2 ... 111)	-0.47 (-0.85 ... -0.15)	59.8 (40.9 ... 71.3)	-0.76 (-0.97 ... -0.47)	77.2 (57.0 ... 93.6)	-0.60 (-0.92 ... -0.39)
CORDEX_MIROC5-RCA4_r1	192 (109 ... 232)	-0.85 (-0.97 ... -0.25)	122 (88.7 ... 149)	-0.70 (-0.97 ... -0.41)	186 (116 ... 235)	-0.76 (-0.97 ... -0.38)
CORDEX_MPI-ESM-LR-RCA4_r1	187 (145 ... 222)	-0.37 (-0.73 ... -0.091)	153 (112 ... 191)	-0.62 (-0.97 ... -0.38)	282 (216 ... 344)	-0.52 (-0.93 ... -0.33)
CORDEX_MPI-ESM-LR-REMO2015_r1	138 (86.6 ... 168)	-0.24 (-0.69 ... 0.22)	176 (106 ... 237)	-0.29 (-0.74 ... 0.17)	264 (196 ... 317)	-0.71 (-0.97 ... -0.36)
CORDEX_NorESM1-M-REMO2015_r1	67.9 (45.3 ... 87.1)	-0.51 (-0.96 ... -0.14)	64.2 (43.0 ... 78.0)	-0.47 (-0.75 ... -0.24)		
HighResMIP						
HighResMIP_CNRM-CM6-1_r1	138 (93.0 ... 162)	-0.65 (-0.96 ... -0.25)	122 (90.1 ... 145)	-0.56 (-0.92 ... -0.32)	136 (90.4 ... 160)	-0.83 (-0.97 ... -0.43)
HighResMIP_CNRM-CM6-1-HR_r1	121 (78.9 ... 150)	-0.67 (-0.96 ... -0.33)	103 (71.9 ... 121)	-0.23 (-0.59 ... 0.0081)	104 (68.7 ... 129)	-0.36 (-0.91 ... -0.0065)
HighResMIP_EC-Earth3P_r1	171 (159 ... 182)	-0.64 (-0.72 ... -0.56)				
HighResMIP_EC-Earth3P_r2	154 (115 ... 185)	-0.59 (-0.83 ... -0.42)	118 (77.4 ... 145)	-0.83 (-0.98 ... -0.53)	146 (106 ... 174)	-0.77 (-0.97 ... -0.43)
HighResMIP_EC-Earth3P_r3	118 (89.7 ... 143)	-0.42 (-0.74 ... -0.20)				
HighResMIP_EC-Earth3P-HR_r1					138 (128 ... 147)	-0.40 (-0.46 ... -0.34)
HighResMIP_EC-Earth3P-HR_r2	123 (92.1 ... 152)	-0.49 (-0.80 ... -0.30)			151 (116 ... 179)	-0.47 (-0.81 ... -0.27)

HighResMIP_EC-Earth3P-HR_r3	106 (77.1 ... 130)	-0.36 (-0.86 ... -0.17)			148 (112 ... 176)	-0.46 (-0.80 ... -0.18)
HighResMIP_HadGEM3-GC31-HM_r1i1	160 (113 ... 194)	-0.63 (-0.94 ... -0.36)	173 (124 ... 207)	-0.88 (-0.98 ... -0.55)	156 (112 ... 190)	-0.65 (-0.95 ... -0.35)
HighResMIP_HadGEM3-GC31-HM_r1i2	122 (84.8 ... 143)	-0.26 (-0.70 ... -0.025)	145 (87.2 ... 159)	-0.94 (-0.97 ... -0.38)		
HighResMIP_HadGEM3-GC31-HM_r1i3	128 (87.9 ... 160)	-0.33 (-0.58 ... -0.071)	130 (95.4 ... 159)	-0.57 (-0.93 ... -0.34)	152 (103 ... 188)	-0.74 (-0.96 ... -0.39)
HighResMIP_HadGEM3-GC31-LM_r1			173 (124 ... 207)	-0.88 (-0.98 ... -0.55)		
HighResMIP_HadGEM3-GC31-MM_r1	141 (90.3 ... 178)	-0.55 (-0.89 ... -0.23)	149 (92.8 ... 178)	-0.68 (-0.97 ... -0.24)	99.6 (69.5 ... 129)	-0.29 (-0.71 ... 0.061)
HighResMIP_MPI-ESM1-2-HR_r1	241 (169 ... 296)	-0.59 (-0.92 ... -0.36)	177 (120 ... 220)	-0.57 (-0.94 ... -0.34)		
HighResMIP_MPI-ESM1-2-XR_r1	125 (76.4 ... 154)	-0.49 (-0.87 ... -0.12)	189 (122 ... 241)	-0.49 (-0.92 ... -0.14)	129 (94.8 ... 159)	-0.29 (-0.68 ... -0.072)

A3 Estimated trends in climate models

This section shows Probability Ratios and change in intensity ΔI for models that passed model evaluation and also includes the values calculated from the fits with observations.

Model / Observations	Jamaica		Lesser Antilles		Puerto Rico	
	Probability ratio	Change in intensity (%)	Probability ratio	Change in intensity (%)	Probability ratio	Change in intensity (%)
CHIRPS	1.1 (0.10 ... ∞)	-0.16 (-20 ... 33)	0.42 (0.33 ... 13)	25 (-24 ... 36)	0.65 (0.12 ... ∞)	1.9 (-32 ... 13)
MSWEP	1.6 (1.4 ... ∞)	-10 (-61 ... -6.0)	1.2 (0.30 ... ∞)	-4.2 (-28 ... 44)	9.0 (0.42 ... ∞)	-19 (-48 ... 8.5)
CORDEX						
CORDEX_CanESM2-CRCM5_r1					∞ (7.2 ... ∞)	-14 (-20 ... -6.8)
CORDEX_CanESM2-RCA4_r1			1.6 (0.88 ... 5.4)	-11 (-26 ... 3.4)	8.4 (1.6 ... ∞)	-18 (-29 ... -4.7)
CORDEX_CNRM-CM5-RCA4_r1	3.3 (0.23 ... ∞)	-9.6 (-25 ... 15)			1.7 (0.66 ... 80)	-8.4 (-27 ... 7.1)
CORDEX_CNRM-CM5-CRCM5_r1			∞ (0.74 ... ∞)	-21 (-28 ... 4.2)	1.7 (0.30 ... ∞)	-4.8 (-23 ... 21)

CORDEX_EC-EARTH-RCA4_r12			1.5 (0.65 ... 7.8)	-9.2 (-28 ... 11)	0.59 (0.22 ... 3.2)	6.6 (-8.3 ... 27)
CORDEX_GFDL-ESM2M-RCA4_r1	12 (0.91 ... ∞)	-22 (-31 ... 1.3)	0.82 (0.36 ... 1.7e+2)	3.5 (-17 ... 25)	0.94 (0.77 ... ∞)	1.0 (-37 ... 3.1)
CORDEX_GFDL-ESM2M-RegCM4-7_r1	0.69 (0.16 ... ∞)	3.0 (-19 ... 20)	0.94 (0.74 ... ∞)	2.0 (-42 ... 10)		
CORDEX_HadGEM2-ES-RCA4_r1	0.84 (0.31 ... 3.1)	2.9 (-14 ... 17)			0.79 (0.31 ... ∞)	5.0 (-20 ... 31)
CORDEX_HadGEM2-ES-RegCM4-7_r1	0.12 (0.062 ... 1.2)	22 (-1.6 ... 38)			1.1 (0.25 ... 4.4)	-2.2 (-38 ... 64)
CORDEX_MIROC5-RCA4_r1	0.13 (0.058 ... 1.3)	33 (-1.3 ... 57)	1.0 (0.43 ... 3.1)	-1.6 (-27 ... 37)	0.61 (0.19 ... 1.7)	16 (-12 ... 65)
CORDEX_MPI-ESM-LR-RCA4_r1	11 (0.76 ... ∞)	-13 (-28 ... 3.5)	2.3 (1.1 ... ∞)	-19 (-43 ... -2.6)	2.5 (0.85 ... ∞)	-15 (-31 ... 2.5)
CORDEX_MPI-ESM-LR-REMO2015_r1	18 (1.4 ... ∞)	-30 (-47 ... -5.7)	3.5 (1.8 ... 1.8e+2)	-27 (-45 ... -16)	∞ (1.8 ... ∞)	-42 (-51 ... -12)
CORDEX_MPI-ESM-MR-RegCM4-7_r1			1.4 (0.41 ... ∞)	-7.6 (-33 ... 39)	7.4 (0.76 ... ∞)	-17 (-30 ... 5.0)
CORDEX_NorESM1-M-RCA4_r1	2.5 (0.25 ... ∞)	-4.6 (-18 ... 11)	0.74 (0.32 ... 2.0)	10 (-16 ... 54)	0.76 (0.18 ... ∞)	4.5 (-21 ... 31)
HighResMIP						
HighResMIP_CNRM-CM6-1_r1	1.4 (0.52 ... ∞)	-8.3 (-36 ... 19)	1.8 (0.55 ... ∞)	-9.1 (-28 ... 16)	0.81 (0.24 ... ∞)	3.9 (-25 ... 31)
HighResMIP_CNRM-CM6-1-HR_r1	∞ (0.87 ... ∞)	-16 (-36 ... 1.0)	0.72 (0.36 ... 1.5)	8.1 (-9.8 ... 30)	1.3 (0.23 ... 7.1e+2)	-3.9 (-25 ... 20)
HighResMIP_EC-Earth3P_r2	2.1 (0.43 ... ∞)	-7.5 (-31 ... 15)	0.92 (0.45 ... ∞)	2.4 (-29 ... 32)		
HighResMIP_EC-Earth3P_r3	2.5 (0.70 ... ∞)	-15 (-31 ... 7.9)				
HighResMIP_EC-Earth3P-HR_r2	∞ (1.2 ... ∞)	-26 (-45 ... -1.9)	1.4 (0.60 ... ∞)	-8.2 (-38 ... 17)	14 (0.55 ... ∞)	-15 (-38 ... 5.5)
HighResMIP_EC-Earth3P-HR_r3	∞ (1.8 ... ∞)	-32 (-41 ... -4.5)			0.78 (0.19 ... ∞)	2.9 (-24 ... 30)
HighResMIP_HadGEM3-GC31-HM_r1i2			1.8 (0.46 ... ∞)	-15 (-40 ... 31)	1.1 (0.11 ... ∞)	-0.40 (-25 ... 22)
HighResMIP_HadGEM3-GC31-HM_r1i3	1.2 (0.21 ... ∞)	-1.7 (-22 ... 24)	0.88 (0.36 ... 8.0)	4.0 (-26 ... 46)	0.34 (0.072 ... ∞)	11 (-12 ... 41)
HighResMIP_HadGEM3-GC31-MM	∞ (0.17 ... ∞)	-15 (-34 ... 22)	1.0 (0.49 ... ∞)	-0.75 (-34 ... 28)	1.9 (0.50 ... ∞)	-9.1 (-27 ... 13)

_r1						
HighResMIP_MPI-ESM1-2-XR_r1	14 (1.0 ... ∞)	-18 (-37 ... -0.24)	0.84 (0.43 ... 2.5)	7.1 (-23 ... 40)	1.0 (0.32 ... ∞)	-0.62 (-24 ... 25)

Table A3.1. Event magnitude, probability ratio and change in intensity for pr-MJJ in each study region for observational datasets and each model that passed the evaluation tests, from pre-industrial climate to the present.

Model / Observations	**Jamaica**		**Lesser Antilles**		**Puerto Rico**	
	Probability ratio	**Change in intensity (mm)**	**Probability ratio**	**Change in intensity (mm)**	**Probability ratio**	**Change in intensity (mm)**
CHIRPS	1.1 (0.074 ... ∞)	0.39 (-80 ... 1.0e+2)	0.71 (0.25 ... ∞)	1.9 (-13 ... 17)	1.3 (0.13 ... ∞)	-8.0 (-1.4e+2 ... 1.2e+2)
MSWEP	∞ (5.2 ... ∞)	3.5e+2 (-6.1e+3 ... 6.5e+3)	0.66 (0.26 ... ∞)	24 (-80 ... 1.3e+2)	3.1 (0.27 ... ∞)	-27 (-2.1e+2 ... 62)
CORDEX						
CORDEX_CanESM2-RCA4_r1	21 (1.5 ... ∞)	-90 (-1.8e+2 ... -18)	3.4 (1.1 ... ∞)	-59 (-1.2e+2 ... -3.2)	∞ (2.5 ... ∞)	-85 (-1.6e+2 ... -24)
CORDEX_CNRM-CM5-RCA4_r1	7.8 (0.12 ... ∞)	-49 (-1.4e+2 ... 97)	5.3 (0.61 ... ∞)	-48 (-1.1e+2 ... 28)	4.4 (0.30 ... ∞)	-64 (-1.7e+2 ... 70)
CORDEX_EC-EARTH-RCA4_r12	0.92 (0.13 ... ∞)	3.1 (-1.2e+2 ... 95)	2.9 (0.71 ... ∞)	-60 (-1.6e+2 ... 26)	0.58 (0.22 ... ∞)	28 (-72 ... 1.2e+2)
CORDEX_GFDL-ESM2M-CRCM5_r1	∞ (6.4 ... ∞)	-91 (-1.5e+2 ... -15)	0.81 (0.39 ... ∞)	6.6 (-34 ... 41)		
CORDEX_GFDL-ESM2M-RegCM4-7_r1					0.80 (0.22 ... ∞)	3.4 (-82 ... 37)
CORDEX_HadGEM2-ES-RCA4_r1	0.65 (0.16 ... ∞)	19 (-67 ... 91)			0.77 (0.25 ... ∞)	8.0 (-51 ... 53)
CORDEX_IPSL-CM5A-MR-RCA4_r1	0.58 (0.14 ... 32)	14 (-38 ... 74)	2.1 (1.0 ... ∞)	-15 (-59 ... -0.024)	∞ (1.3 ... ∞)	-35 (-64 ... -2.4)
CORDEX_MIROC5-RCA4_r1	0.27 (0.049 ... ∞)	61 (-21 ... 2.4e+2)	0.97 (0.44 ... 5.1)	2.0 (-69 ... 66)	0.33 (0.13 ... 1.4)	73 (-12 ... 1.7e+2)
CORDEX_MPI-ESM-LR-RCA4_r1	0.64 (0.15 ... ∞)	22 (-1.2e+2 ... 1.3e+2)	1.7 (0.61 ... ∞)	-30 (-96 ... 40)		
CORDEX_MPI-ESM-LR-REMO2015_r1	2.1e+2 (2.9 ... ∞)	-1.5e+2 (-3.2e+2 ... -46)	74 (4.6 ... ∞)	-2.6e+2 (-4.6e+2 ... -1.5e+2)		
CORDEX_NorESM1-M-REMO2015			0.45 (0.22 ... 12)	39 (-35 ... 1.1e+2)		

_r1						
HighResMIP						
HighResMIP_CNRM-CM6-1_r1	9.5 (0.29 ... ∞)	-33 (-1.2e+2 ... 42)	7.8 (0.79 ... ∞)	-57 (-1.3e+2 ... 13)	0.70 (0.099 ... ∞)	9.0 (-82 ... 82)
HighResMIP_CNRM-CM6-1-HR_r1	∞ (0.64 ... ∞)	-63 (-1.4e+2 ... 6.9)	0.77 (0.34 ... 2.2)	23 (-60 ... 1.1e+2)	3.7 (0.11 ... ∞)	-27 (-1.2e+2 ... 56)
HighResMIP_EC-Earth3P_r1	1.3 (1.0 ... 1.9)	-6.3 (-13 ... -0.15)				
HighResMIP_EC-Earth3P_r2	0.81 (0.43 ... ∞)	5.3 (-1.6e+2 ... 28)	0.94 (0.40 ... ∞)	2.7 (-66 ... 63)	∞ (0.098 ... ∞)	-44 (-97 ... 43)
HighResMIP_EC-Earth3P_r3	4.5 (0.52 ... ∞)	-43 (-1.6e+2 ... 28)				
HighResMIP_EC-Earth3P-HR_r1					1.2 (0.91 ... 1.7)	-6.6 (-17 ... 3.5)
HighResMIP_EC-Earth3P-HR_r2	∞ (6.8 ... ∞)	-1.4e+2 (-2.7e+2 ... -31)			0.74 (0.40 ... ∞)	7.8 (-2.0e+2 ... 23)
HighResMIP_EC-Earth3P-HR_r3	∞ (1.8 ... ∞)	-1.4e+2 (-2.4e+2 ... -11)			7.3 (0.16 ... ∞)	-30 (-1.3e+2 ... 85)
HighResMIP_HadGEM3-GC31-HM_r1i1	∞ (0.76 ... ∞)	-99 (-1.9e+2 ... 9.6)			23 (0.075 ... ∞)	-21 (-1.1e+2 ... 82)
HighResMIP_HadGEM3-GC31-HM_r1i2	18 (0.49 ... ∞)	-81 (-1.8e+2 ... 31)	93 (0.53 ... ∞)	-68 (-1.3e+2 ... 41)		
HighResMIP_HadGEM3-GC31-HM_r1i3	1.6 (0.18 ... ∞)	-16 (-1.3e+2 ... 93)	1.4 (0.36 ... ∞)	-16 (-71 ... 83)	0.12 (0.039 ... ∞)	71 (-52 ... 1.6e+2)
HighResMIP_HadGEM3-GC31-LM_r1			∞ (0.45 ... ∞)	-63 (-1.0e+2 ... 65)		
HighResMIP_HadGEM3-GC31-MM_r1	0.96 (0.12 ... ∞)	0.89 (-1.4e+2 ... 80)	92 (0.76 ... ∞)	-84 (-1.7e+2 ... 21)	6.0 (0.39 ... ∞)	-35 (-1.4e+2 ... 34)
HighResMIP_MPI-ESM1-2-HR_r1	∞ (0.99 ... ∞)	-2.0e+2 (-4.1e+2 ... 0.54)	1.6 (0.73 ... ∞)	-36 (-2.0e+2 ... 36)		
HighResMIP_MPI-ESM1-2-XR_r1	∞ (11 ... ∞)	-1.4e+2 (-2.3e+2 ... -34)	1.3 (0.47 ... ∞)	-22 (-1.9e+2 ... 1.0e+2)	0.89 (0.14 ... ∞)	3.9 (-1.4e+2 ... 87)

Table A3.1. Event magnitude, probability ratio and change in intensity for eff-pr-MJJ in each study region for observational datasets and each model that passed the evaluation tests, from pre-industrial climate to the present.